Electronic Supplementary Material (ESI) for ChemComm.

Supporting Information

Synthesis and Aqueous Anion Recognition of Imidazolium-Based Nonacationic Cup

Pinpin Wang,[a,b] Kai Liu,[c] Huanqing Ma,[b] Hao Nian,[b] Yawen Li,[b] Qingfang Li,[b] Lin Cheng,[b] and Liping Cao[b,*]

[a]College of Food Science and Pharmaceutical Engineering, Zaozhuang University, Zaozhuang 277160, P. R. China.

[b]College of Chemistry and Materials Science, Northwest University, Xi'an 710069, P. R. China.

[c]Institute of Marine Drugs, Guangxi University of Chinese Medicine, Nanning 530200.

*E-mail: chcaoliping@nwu.edu.cn

Table of Contents **Pages**

Experimental Procedures

General Experimental Details. Starting materials were purchased from commercial suppliers were used without further purification. Melting points were recorded by using a XT-4 apparatus in open capillary tubes. IR spectra were measured on a TENSOR27 spectrometer. NMR spectra were recorded on a spectrometer operating at 400 MHz and 600 MHz for ^{1}H NMR, 100 MHz and 150 MHz for ^{13}C NMR spectra on Bruker ascend^{TM} 400 spectrometer, JEOL 400 and JEOL 600 spectrometer. Electrospray Ionization (ESI) mass spectra were acquired with Ultimate 3000 electrospray instrument. Fluorescence spectra were performed by using a Horiba Fluorolog-3 spectrometer and QuantaMaster 8000. Isothermal titration calorimetry (ITC) was carried out using a VP-ITC (Malvern) at 25 ˚C, and computer fitting of the data were performed using the VP-ITC analyze software. UV/vis spectra were done on Agilent Cary-100 spectrometer. X-ray diffraction data collection of the compounds were recorded by Bruker D8 Venture photon II diffractometer.

Synthetic Procedures and Characterization Data

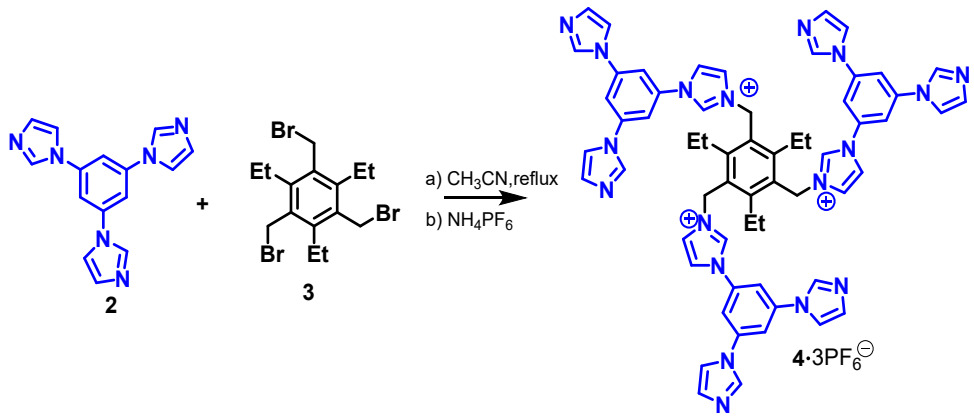

Compound 4•3PF$_6^-$. **2** (310 mg, 1.12 mmol) was added to dry MeCN (120 mL) in two-necked flask and the suspension was heated at 95°C until all compounds were dissolved. **3** (83 mg, 0.19 mmol) was dissolved in MeCN (20 mL) and slowly added to the solution of **3,** then mixture reacted at 95 ℃ for another 2 days. The mixture was cooled to room temperature, and the precipitate was collected and washed with an excess amount of acetone (3 × 30 mL) by centrifuge to give crude product with Br$^-$

counterions as a white solid. Crude product was dissolved in H_2O (20 mL) and excess amount of NH_4PF_6 was added with stirring for 12 h. The precipitate was collected and washed with an excess amount of H_2O (3 × 30 mL) to give **4**•3PF_6^- as a white solid (189 mg, 69%). M.p. > 300 °C. IR (KBr, cm^{-1}): 3430w, 1617s, 1556m, 1508m, 1258m, 1190m, 1069m, 842s, 556s. ^{1}H NMR (400 MHz, CD_3CN): 8.84 (s, 3H), 8.27 (s, 6H), 7.95-7.90 (m, 6H), 7.77 (d, J = 1.8, 6H), 7.68 (s, 6H), 7.52 (t, J = 1.8, 3H), 7.27 (s, 6H), 5.62 (s, 6H), 2.76 (q, J = 7.3, 6H), 1.14 (t, J = 7.3, 9H). ^{13}C NMR (150 MHz, CD_3CN): 149.2, 139.3, 136.8, 134.7, 129.3, 128.1, 123.4, 122.4, 118.9, 115.4, 114.2, 48.0, 23.7, 14.8 (only 14 of the 15 resonances expected were observed). ESI-TOF-MS: m/z 343.1629 ([**4**•3PF_6^--3PF_6^-]$^{3+}$, calcd. for $[C_{60}H_{57}N_{18}]^{3+}$, 343.1665); 587.2249 ([**4**•3PF_6^--2PF_6^-]$^{2+}$, calcd. for $[C_{60}H_{57}N_{18}PF_6]^{2+}$, 587.2322).

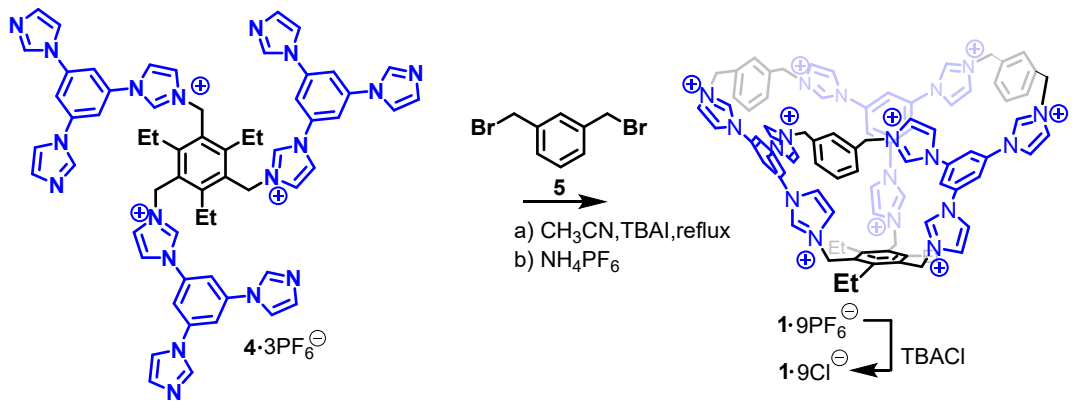

Compound 1•9PF_6^-. **4**•3PF_6^- (148 mg, 0.101 mmol) and **5** (98 mg, 0.33 mmol) was added to dry MeCN (100 mL) in pressure flask, then mixture reacted at 110 ℃ for 3 days. The mixture was cooled to room temperature, and the mixture was evaporated by rotation. Crude product was dissolved in H_2O (30 mL) and excess amount of NH_4PF_6 was added with stirring for 12 h. The precipitate was collected and washed with an excess amount of H_2O (3 × 30 mL) to give **1**•9PF_6^-. The crude product was purified by silica gel chromatography with CH_2Cl_2: MeCN (saturated NH_4PF_6) = 3:1 (v:v) and washed with an excess amount of H_2O (3 × 2 mL) to give a white solid (22 mg, 16%). M.p. > 300 °C. IR (KBr, cm^{-1}): 3652m, 3432w, 3156m, 1622s, 1553s, 1508m, 1450m, 1181m, 1092m, 838s, 556s. ^{1}H NMR (400 MHz, CD_3CN): 8.83 (s, 6H), 8.53 (s, 3H), 7.97 (t, J = 1.9, 3H), 7.90 (d, J = 1.9, 6H), 7.78 (t, J = 1.9, 6H), 7.70-7.55 (m, 21H),

7.46 (s, 3H), 5.56 (s, 6H), 5.47 (d, J = 14.7, 6H), 5.43 (d, J = 14.7, 6H), 2.79 (q, J =7.3, 6H), 1.26 (t, J =7.3, 9H). ^{13}C NMR (150 MHz, CD_3CN): 148.6, 148.8, 136.2, 134.8, 133.9, 133.4, 130.6, 130.1, 129.5, 128.0, 124.3, 123.7, 122.7, 121.7, 120.2, 119.0, 53.1, 47.9, 23.5, 14.5. ESI-TOF-MS: m/z 384.3131 ([**1**•9PF_6^--5PF_6^-]$^{5+}$, calcd. for [$C_{84}H_{81}N_{18}P_4F_{24}$]$^{5+}$, 384.3086); 516.6328 ([**1**•9PF_6^--4PF_6^-]$^{4+}$, calcd. for [$C_{84}H_{81}N_{18}P_5F_{30}$]$^{4+}$, 516.6270); 737.1642 ([**1**•9PF_6^--3PF_6^-]$^{3+}$, calcd. for [$C_{84}H_{81}N_{18}P_6F_{36}$]$^{3+}$, 737.1575); 1178.2341 ([**1**•9PF_6^--2PF_6^-]$^{2+}$, calcd. for [$C_{84}H_{81}N_{18}P_7F_{42}$]$^{2+}$, 1178.2187).

Compound 1•9Cl$^-$. The solution of **1**•9PF_6^- (15 mg, 5.6 μmol) in MeCN (2 mL) was added 20 equiv of tetrabutylammonium chloride hydrate (31 mg, 11.2 μmol), then the mixture was stirred for another 12h. The precipitate was collected and washed with an excess amount of MeCN (3 × 2 mL) to give 1•8Cl^- as a white solid (8.7 mg, 83%). M.p. > 300 °C. IR (KBr, cm^{-1}): 3432w, 3074m, 1622s, 1553s, 1484m, 1443m, 1360m,1333m, 1181s, 1092s, 844m, 755m, 638m. ^{1}H NMR (400 MHz, D_2O): 8.18 (t, J = 2.0, 3H), 8.08 (d, J = 2.0, 6H), 8.00 (d, J = 2.0, 6H), 7.94 (d, J = 1.6, 3H), 7.88 (d, J = 2.0, 3H), 7.76 (d, J = 1.6, 6H), 7.70-7.60 (m, 9H), 7.47 (s, 3H), 5.70 (s, 6H), 5.60 (d, J = 14.8, 6H), 5.56 (d, J = 14.8, 6H), 2.86 (q, J = 7.3, 6H), 1.31 (t, J =7.3, 9H) (the resonances for imidazolium H_i and H_d were disappeared owing to the exchange with D atom in D_2O). ^{1}H NMR (400 MHz, DMSO-d_6): 10.70 (s, 6H), 10.04 (s, 3H), 8.99 (s, 3H), 8.78 (s. 6H), 8.73 (s, 3H), 8.51 (s, 6H), 8.36 (s, 3H), 8.26 (s, 6H), 7.91 (s, 3H), 7.49 (d, J = 7.6, 6H), 7.51 (t, J = 7.6, 3H), 5.65 (d, J = 14.7, 6H), 5.61 (s, 6H), 5.55 (d, J = 14.7, 6H), 3.00-2.80 (m, 6H), 1.15-1.00 (m, 9H). ^{13}C NMR (100 MHz, CD_3CN): 145.9, 134.2, 134.0, 131.1, 127.9, 127.7, 126.0, 125.4, 121.5, 120.8, 120.4, 119.2, 116.9, 115.8, 50.5, 45.2, 21.4, 12.0 (only 18 of the 20 resonances expected were observed). ESI-TOF-MS: m/z 296.7177 ([**1**•9Cl^--5Cl^-]$^{5+}$, calcd. for [$C_{84}H_{81}N_{18}$ Cl_4]$^{5+}$, 296.7123); 379.6348 ([**1**•9Cl^--4Cl^-]$^{4+}$, calcd. for [$C_{84}H_{81}N_{18}Cl_5$]$^{4+}$, 379.6326); 517.8205 ([**1**•9Cl^--3Cl^-]$^{3+}$, calcd. for [$C_{84}H_{81}N_{18}Cl_6$]$^{3+}$, 517.1669); 795.2132 ([**1**•9Cl-2Cl^-]$^{2+}$, calcd. for [$C_{84}H_{81}N_{18}Cl_7$]$^{2+}$, 795.2335).

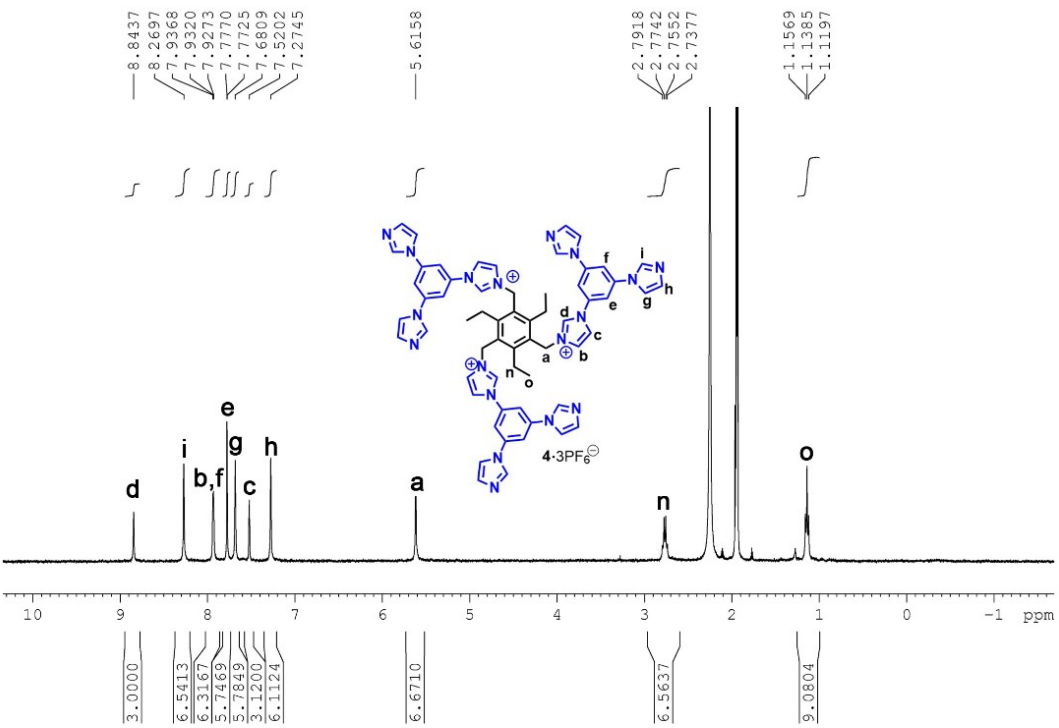

Fig. S1 ^{1}H NMR spectrum recorded (400 MHz, CD_3CN, RT) for **4**•3PF_6^-.

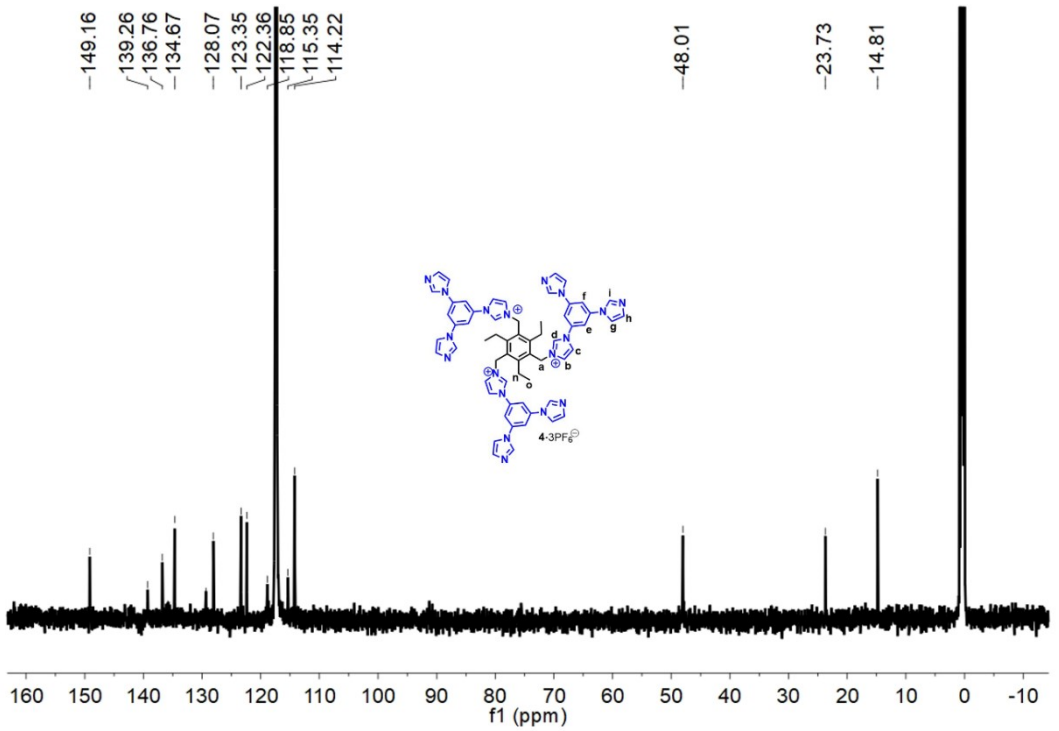

Fig. S2 ^{13}C NMR spectrum recorded (150 MHz, CD_3CN, RT) for **4**•3PF_6^-.

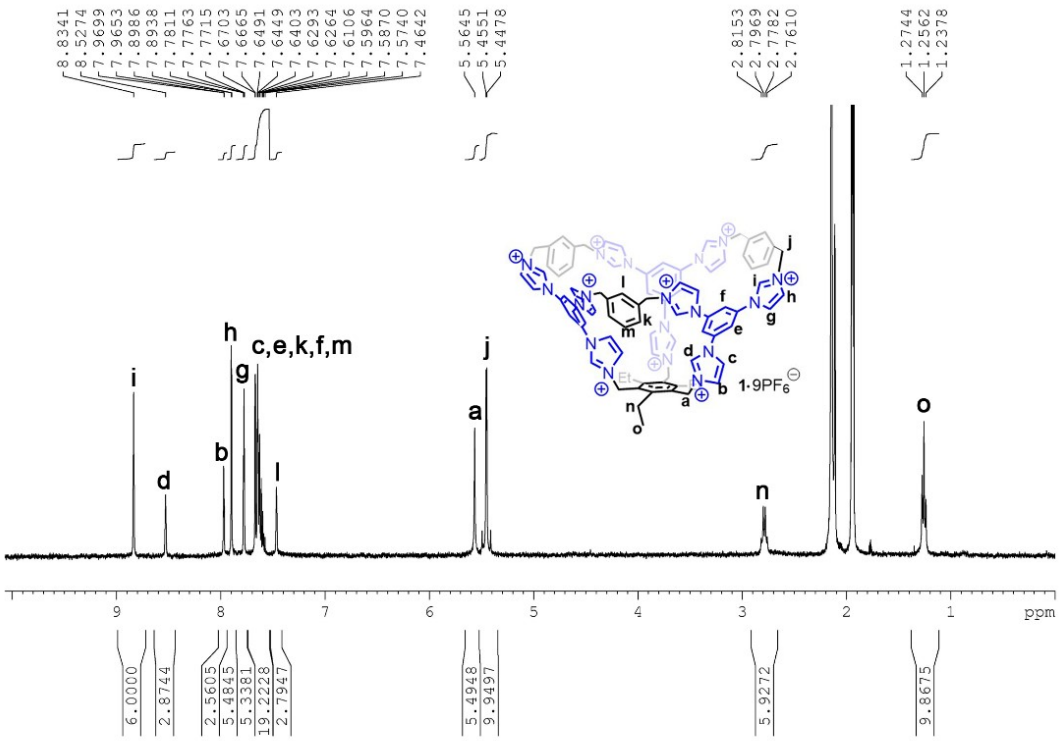

Fig. S3 ^{1}H NMR spectrum recorded (400 MHz, CD_3CN, RT) for **1**•9PF_6^-.

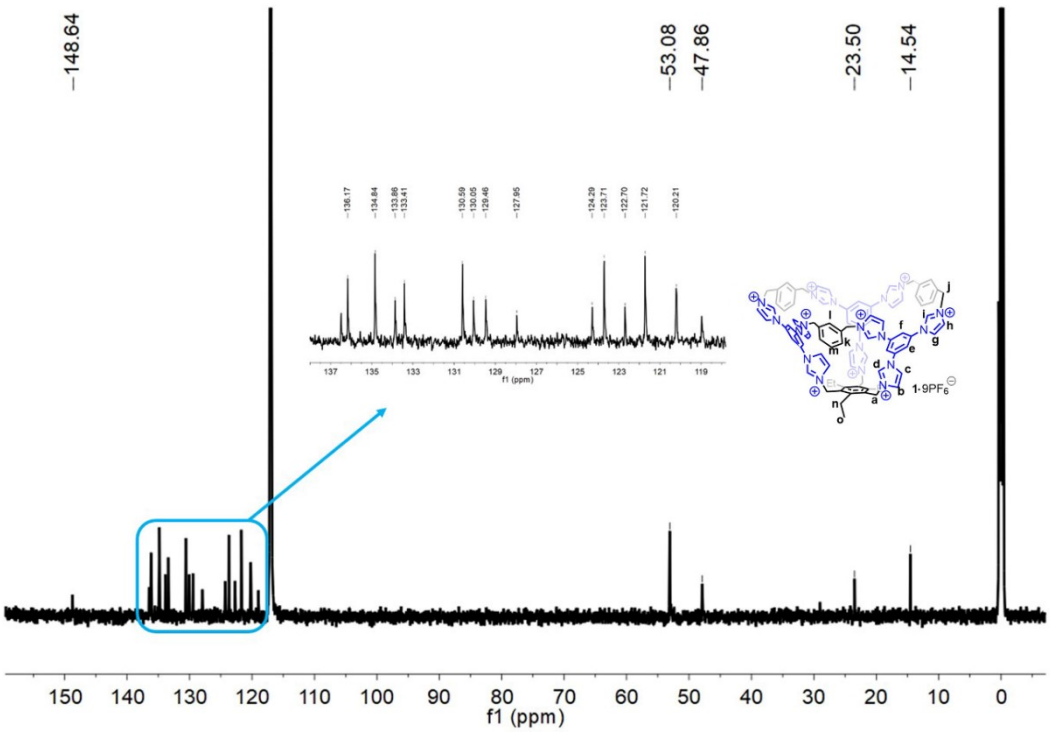

Fig. S4 ^{13}C NMR spectrum recorded (150 MHz, CD_3CN, RT) for **1**•9PF_6^-.

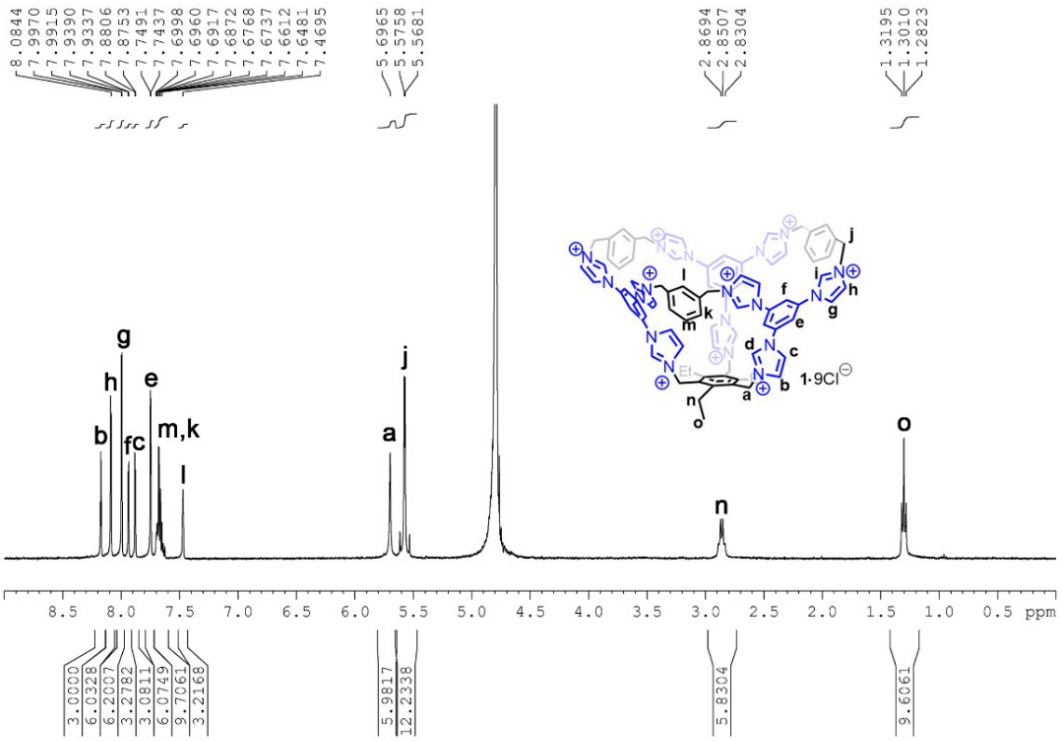

Fig. S5 ^{1}H NMR spectrum recorded (400 MHz, D_2O, RT) for **1**•9Cl$^-$.

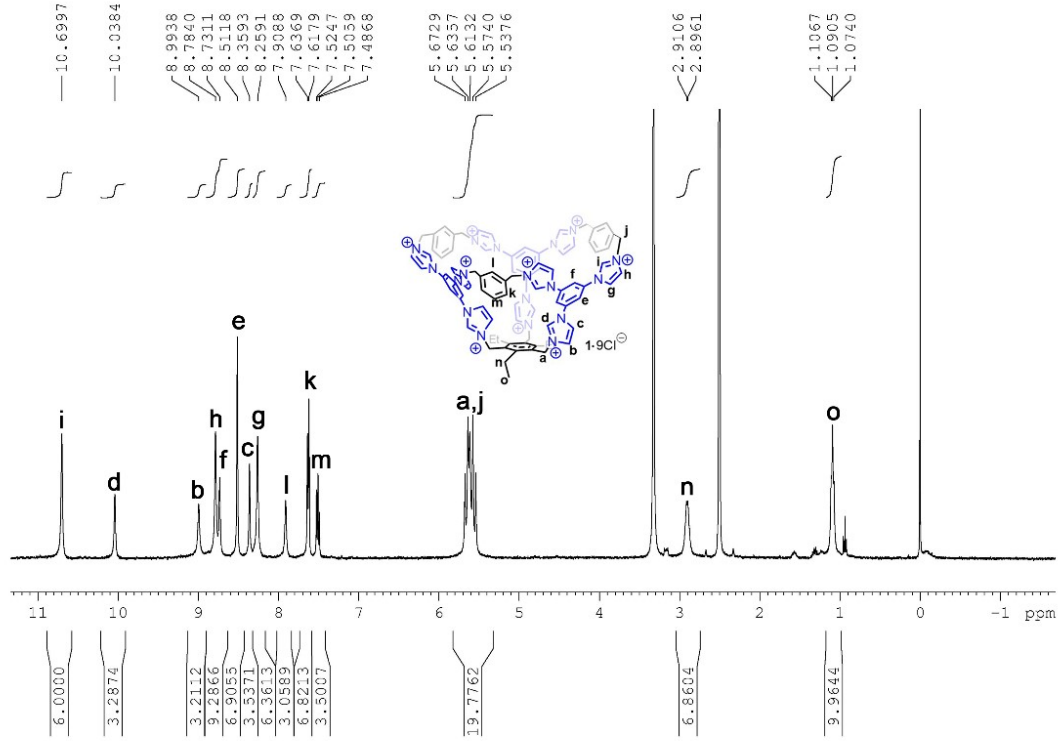

Fig. S6 ^{1}H NMR spectrum recorded (400 MHz, DMSO-d_6, RT) for **1**•9Cl$^-$.

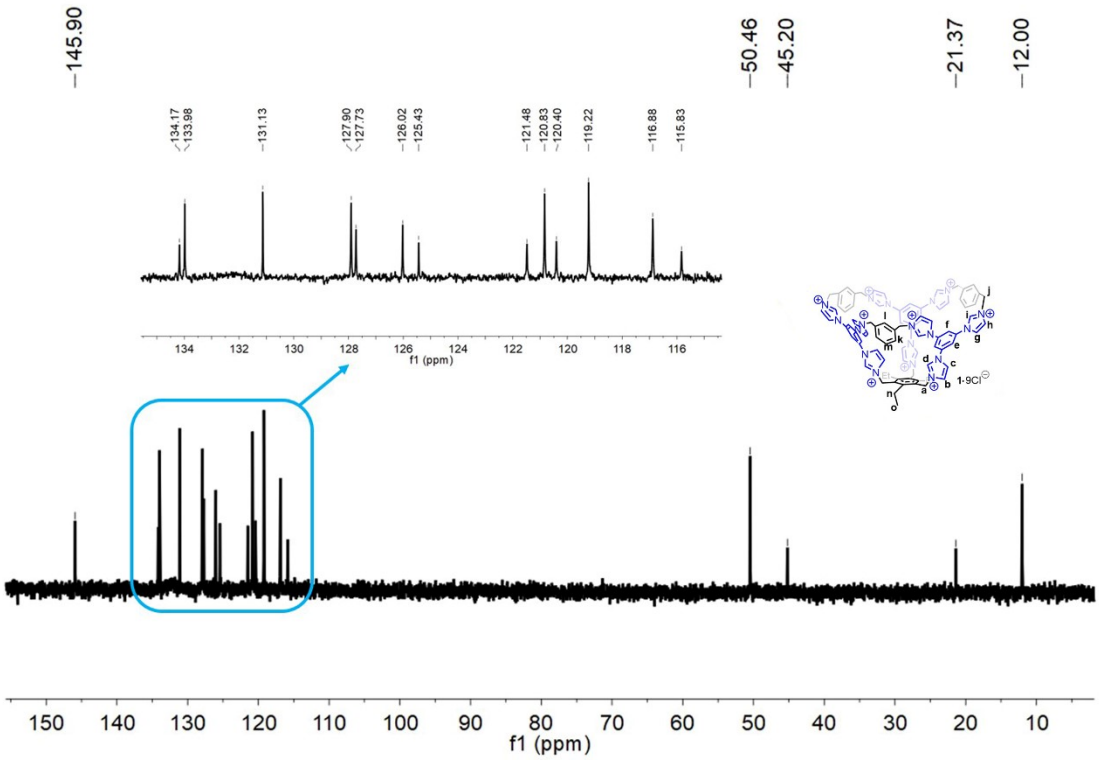

Fig. S7 ^{13}C NMR spectrum recorded (100 MHz, D_2O, RT) for **1**•9Cl^-.

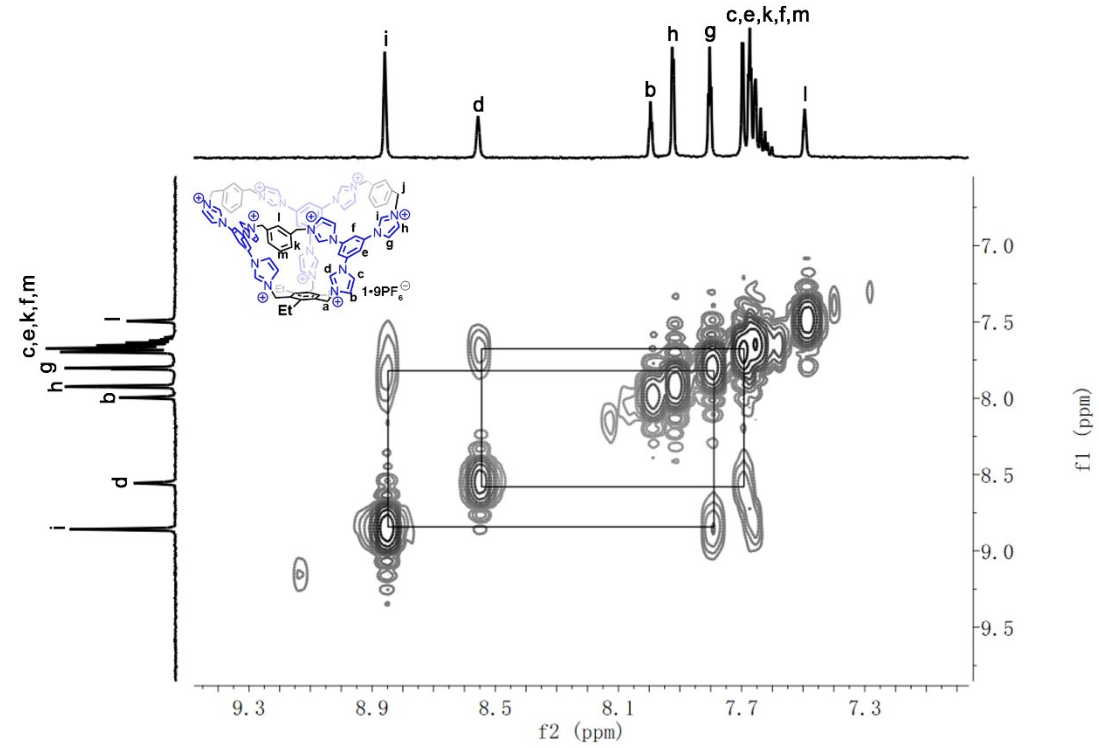

Fig. S8 COSY spectrum recorded (400 MHz, CD_3CN, RT) for **1**•9PF_6^-.

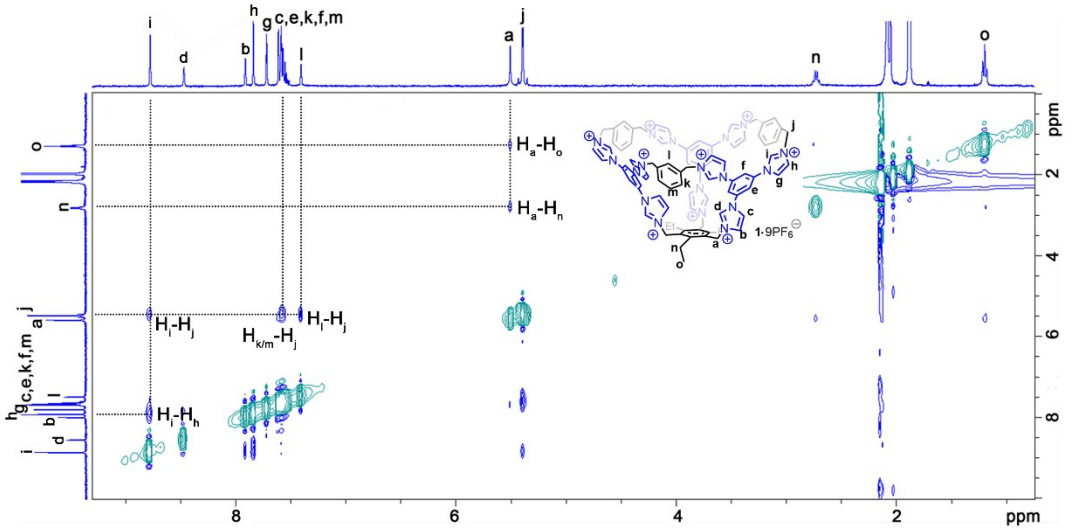

Fig. S9 NOESY spectrum recorded (400 MHz, CD_3CN, RT) for **1**•9PF_6^-.

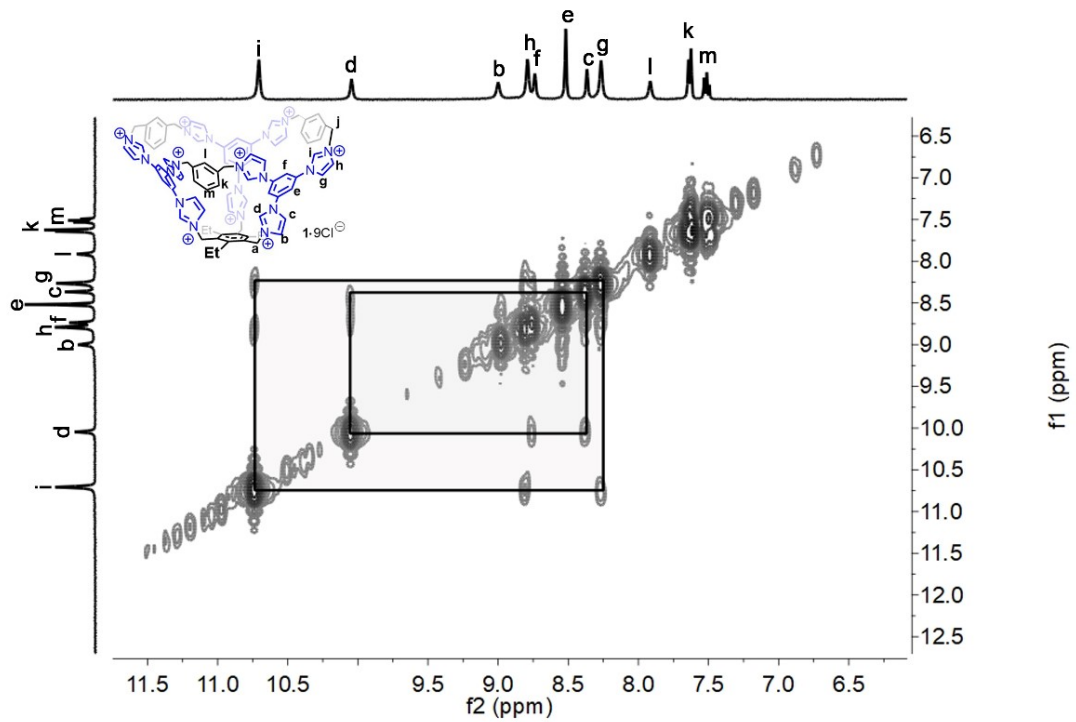

Fig. S10 COSY spectrum recorded (400 MHz, DMSO-d_6, RT) for **1**•9Cl^-.

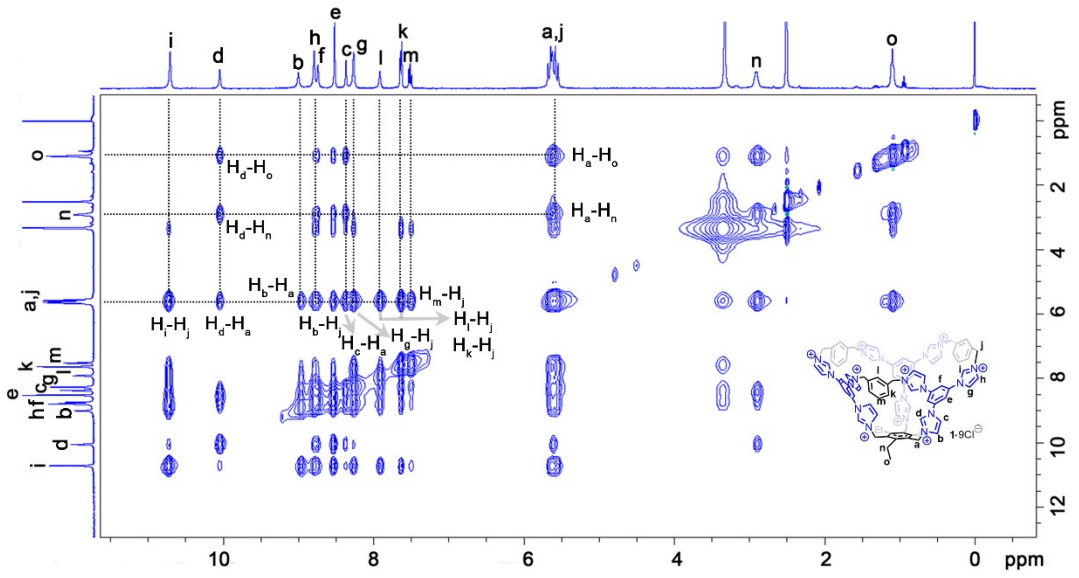

Fig. S11 NOESY spectrum recorded (400 MHz, DMSO-d_6, RT) for **1**•9Cl$^-$.

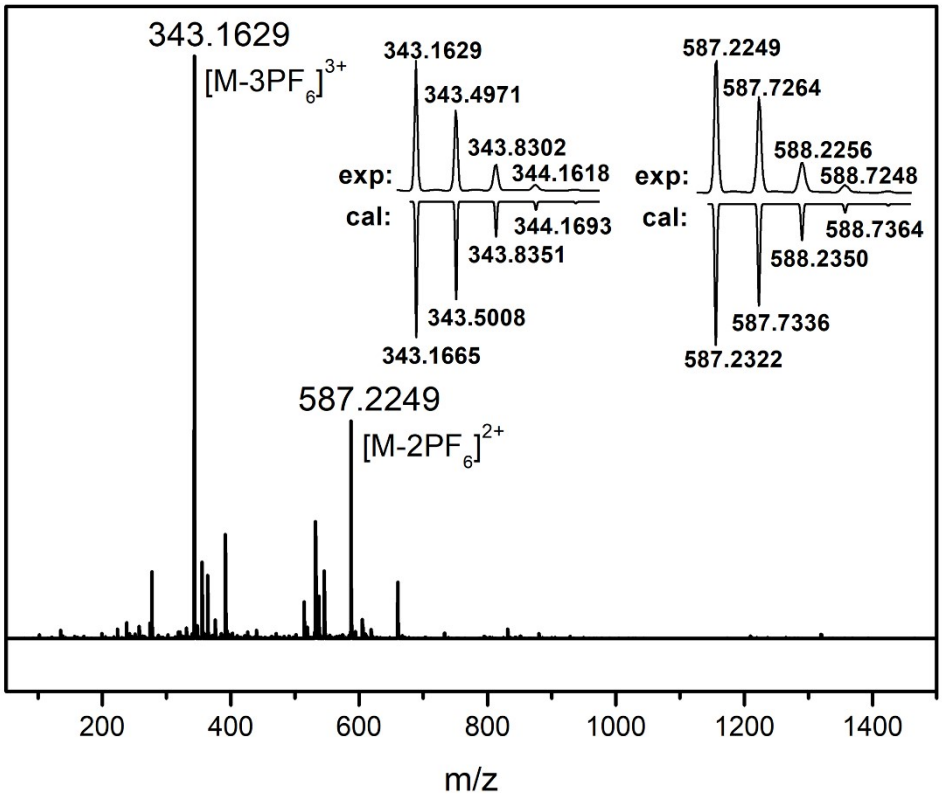

Fig. S12 ESI-MS spectrum of **4**•3PF_6^-.

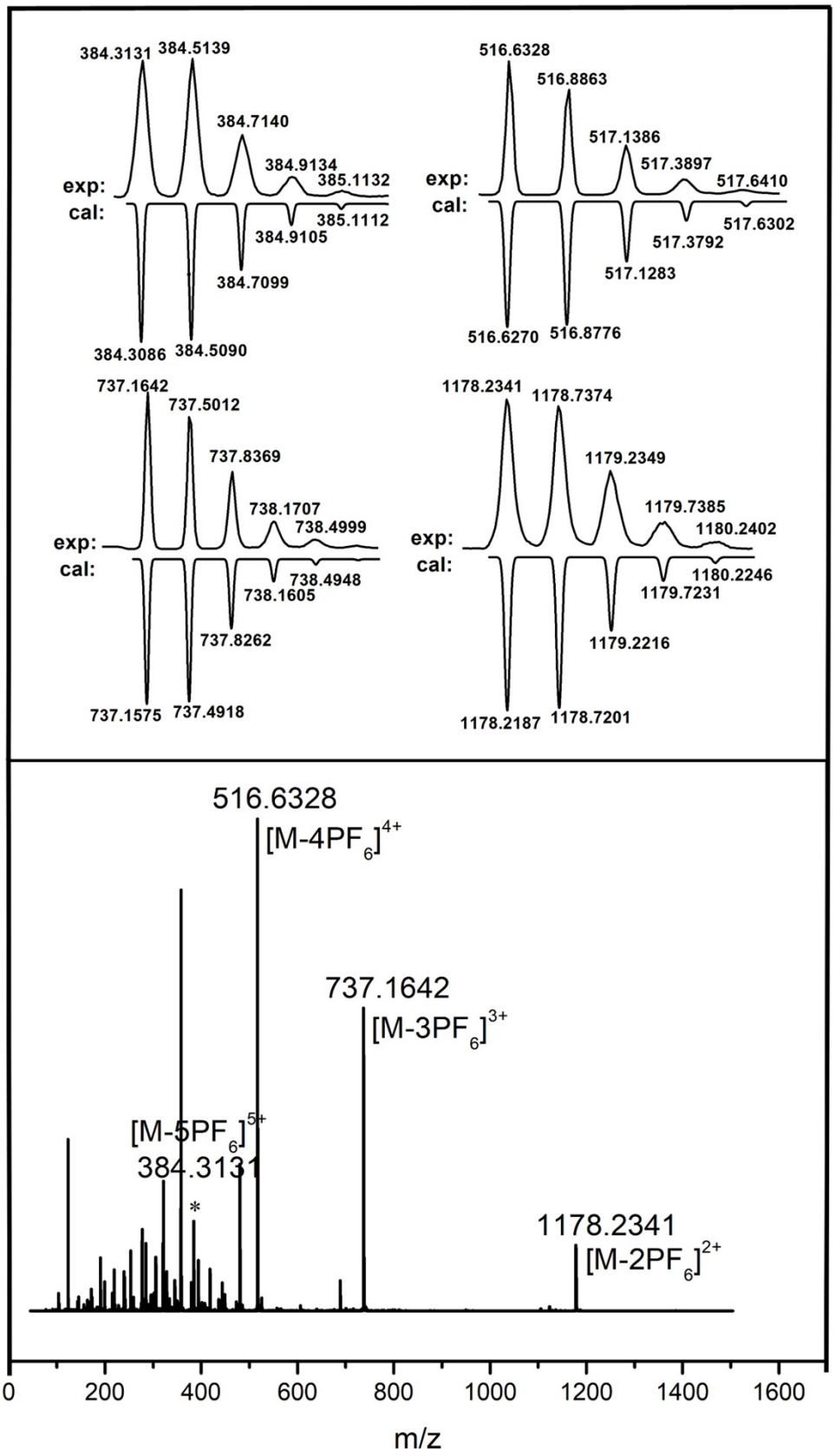

Fig. S13 ESI-MS spectrum of **1**•9PF_6^-.

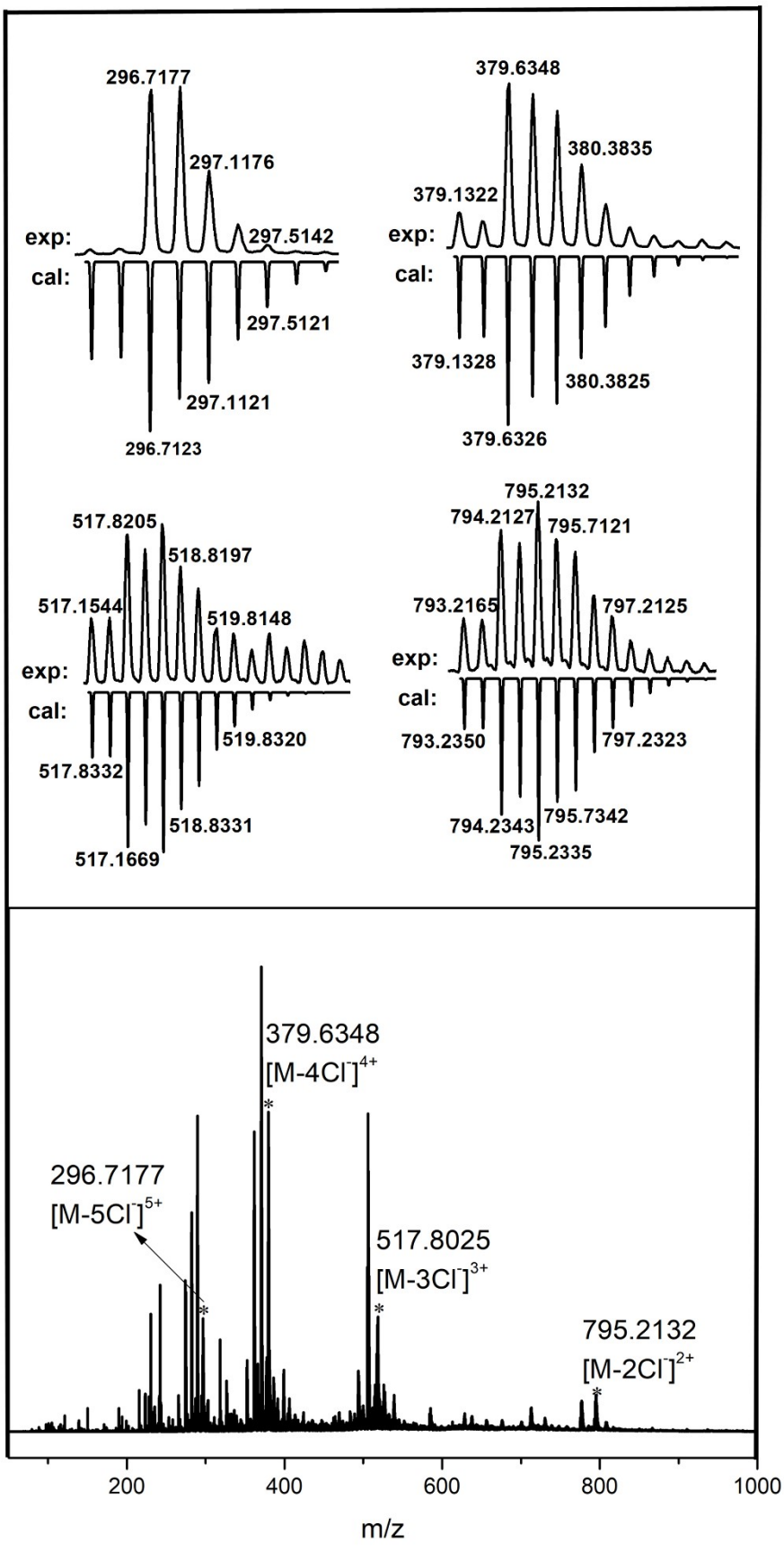

Fig. S14 ESI-MS spectrum of **1**•9Cl^-.

X-ray Structure determination

X-ray diffraction data collection of the compounds were recorded by Bruker VENTURE system with PHOTON II CPAD detector equipped at 150 K and a Ga-target Liquid METALJET D2 PLUS X-ray Source (λ = 1.34139 Å). The structure was solved by SHELXT (version 2018/2) and refined by full-matrix least-squares procedures using the SHELXL program (version 2018/3) through the OLEX2 graphical interface.

1•9PF_6^- (2.67 mg, 0.5 mmol) was dissolved in CH_3CN (2 mL) and the solution was passed through a 0.45 μm filter into a 10 mL tube, which was placed inside a 500 mL wild-mouth bottle containing dichloromethane (50 mL). The bottle was capped, after slow evaporation of dichloromethane at 5℃ into the CH_3CN solution for 7 day, and colorless single crystals of **1**•9PF_6^-were obtained.

1•9Cl^- (1.68 mg, 0.5 mmol) was dissolved in MeOH (2 mL) and the solution was passed through a 0.45 μm filter into a 10 mL tube, which was placed inside a 500 mL wild-mouth bottle containing dichloromethane (50 mL). The bottle was capped, after slow evaporation of dichloromethane at 5℃ into the MeOH solution for 7 day, and colorless single crystals of **1**•9Cl^- were obtained.

Table S1. Crystal data and structure refinement for **1**•9Cl^-

Empirical formula	C117 H131 Cl2 F54 N34 P9
Formula weight	3389.18
Temperature	90 K
Wavelength	1.34138 A
Crystal system, space group	Triclinic, P-1
Unit cell dimensions	a = 15.8416(16) Å α = 95.115(4)° b = 16.8382(17) Å β = 99.575(3)° c = 27.118(3) Å γ = 94.411(4)°
Volume	7073.2(12) Å^3
Z, Calculated density	2, 1.591 Mg/m^3
Absorption coefficient	1.658 mm^-1
F (000)	3452.0
Crystal size	0.16 × 0.14 × 0.09 mm
Theta range for data collection	2.588 to 55.181°

Limiting indices	-19<=h<=19, -20<=k<=20, -33<=l<=32
Reflections collected / unique	150955 / 26946 [R(int) = 0.0587]
Completeness to θ = 53.594	99.7 %
Absorption correction	Semi-empirical from equivalents
Max. and min. transmission	0.7632 and 0.6132
Refinement method	Full-matrix least-squares on F^2
Data / restraints / parameters	26946 / 4774 / 2084
Goodness-of-fit on F^2	1.031
Final R indices [I>2sigma(I)]	R1 = 0.0775, wR2 = 0.2128
R indices (all data)	R1 = 0.0860, wR2 = 0.2193
Extinction coefficient	n/a
Largest diff. peak and hole	1.303 and -0.698 e. Å^-3

Table S2. Crystal data and structure refinement for **1**•9Cl^-

Empirical formula	C93 H99 Cl27 N18
Formula weight	2426.05
Temperature	150(2) K
Wavelength	1.34139 A
Crystal system, space group	Monoclinic, P 1 21/n 1
Unit cell dimensions	a = 16.3833(6) Å α =90° b = 20.8000(8) Å β = 95.615(2)° c = 37.6802(15) Å γ = 90°
Volume	12778.8(8) Å^3
Z, Calculated density	4, 1.261 Mg/m^3
Absorption coefficient	3.686 mm^-1
F (000)	4968
Crystal size	0.4 × 0.3 × 0.2 mm
Theta range for data collection	2.050 to 52.998°
Limiting indices	-19<=h<=19, -24<=k<=24, -44<=l<=44
Reflections collected / unique	185754 / 22518 [R(int) = 0.1921]
Completeness to θ = 53.594	99.6 %
Absorption correction	Semi-empirical from equivalents
Max. and min. transmission	0.7365 and 0.4620
Refinement method	Full-matrix least-squares on F^2
Data / restraints / parameters	22518 / 1 / 1027
Goodness-of-fit on F^2	1.686

Final R indices [I>2sigma(I)]	R1 = 0.1187, wR2 = 0.3759
R indices (all data)	R1 = 0.1274, wR2 = 0.3936
Extinction coefficient	n/a
Largest diff. peak and hole	1.698 and -1.157 e. Å^-3

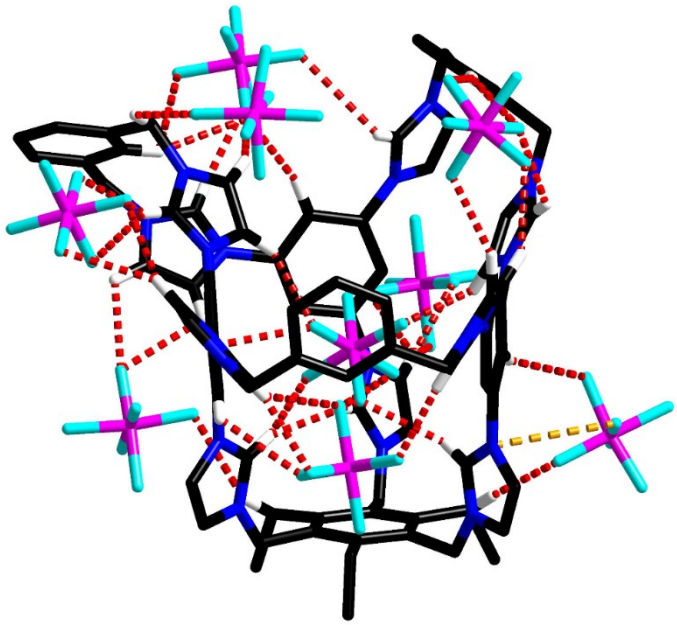

Fig. S15 The C–H···F^- (2.217-2.896 Å) and N^+···F^- (3.465 Å) interactions between F ions and the acidic CH/positive-charged N^+ of imidazolium groups in the X-ray crystal structure of **1**•9PF_6^-. Dash line: Hydrogen bonds (red) and electrostatic interactions (yellow).

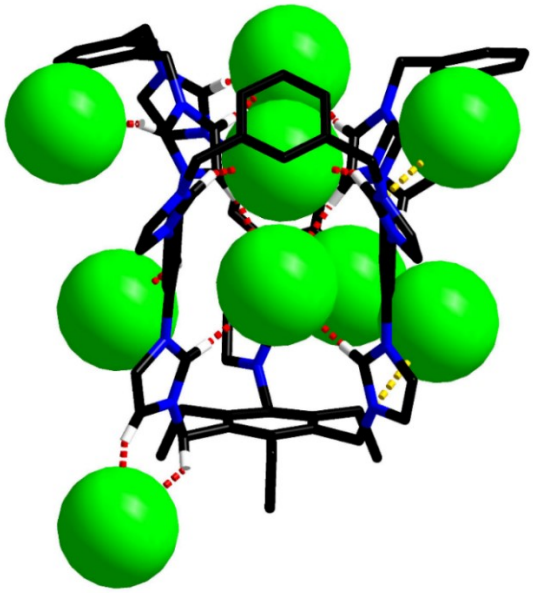

Fig. S16 The C–H···Cl^- and N^+···Cl^- interactions between Cl ions and the acidic CH/positive-charged N^+ of imidazolium groups in the X-ray crystal structure of **1**•9Cl^-. Dash line: Hydrogen bonds (red) and electrostatic interactions (yellow).

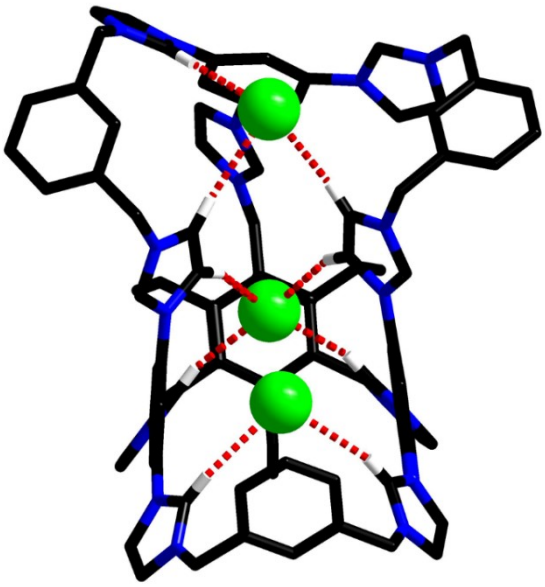

Fig. S17 The C–H···Cl^- interactions between Cl ions and the acidic CH of imidazolium groups in the X-ray crystal structure of **1**•9Cl^-. Dash line: Hydrogen bonds (red).

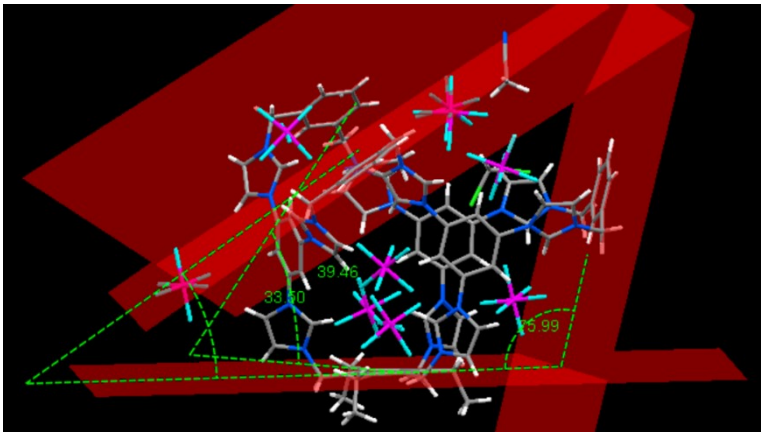

Fig. S18 The angle of three benzene rings in the X-ray crystal structure of **1**•9PF_6^-.

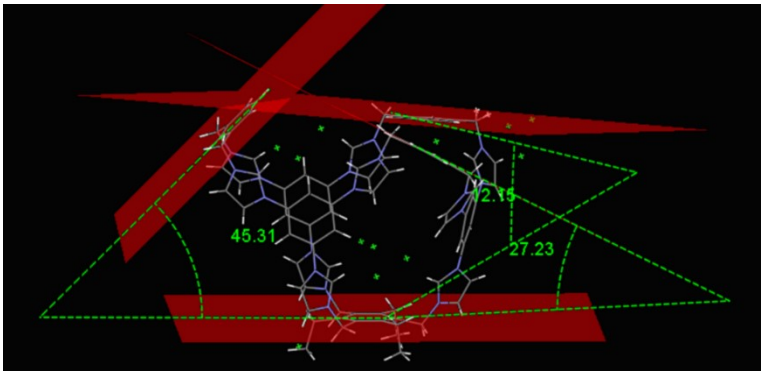

Fig. S19 The angle of three benzene rings in the X-ray crystal structure of **1**•9Cl^-.

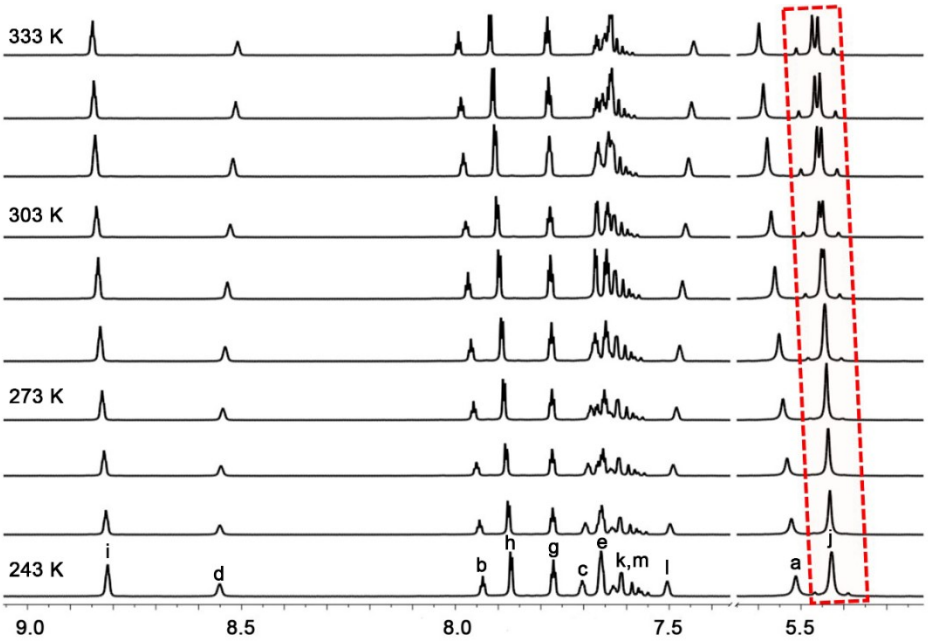

Fig S20. ^{1}H NMR spectrum (400 MHz, CD_3CN, 243K-333K) of **1**•9PF_6^-.

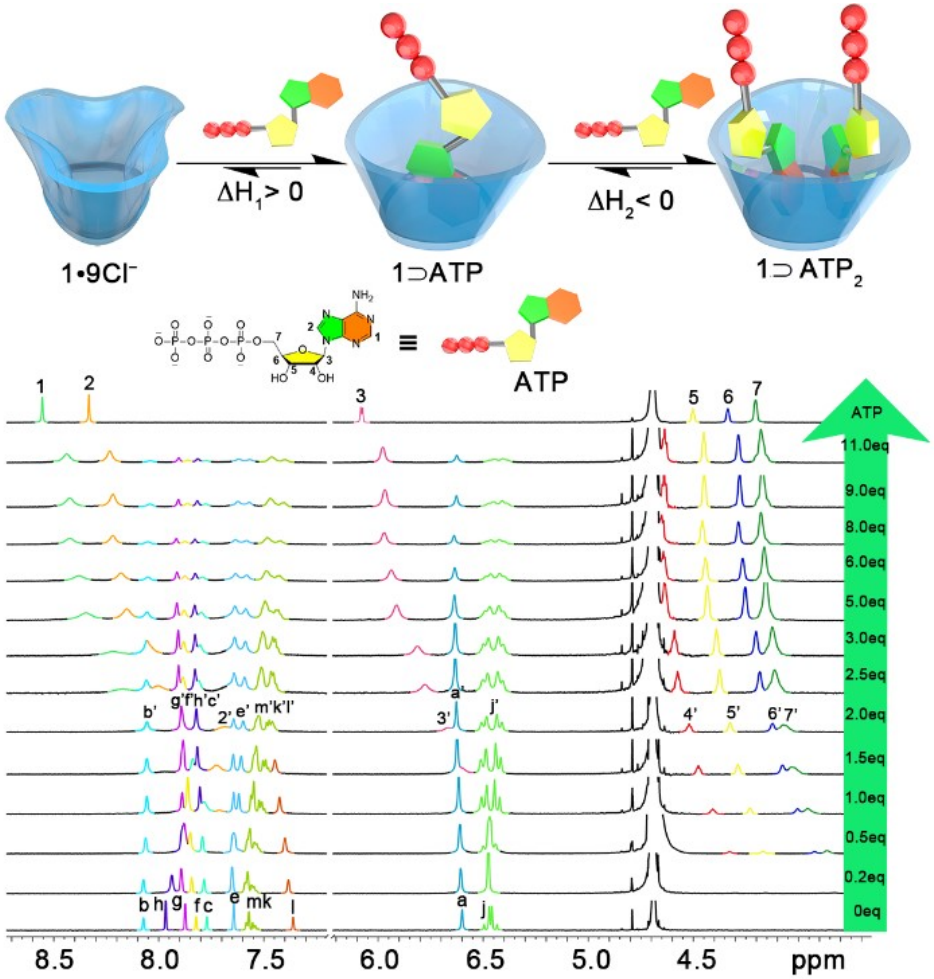

Fig. S21 ^{1}H NMR titration (600 MHz, RT, D_2O) of **1**•9Cl^- (1.0 mM) titrated by ATP (0-11.0 equiv).

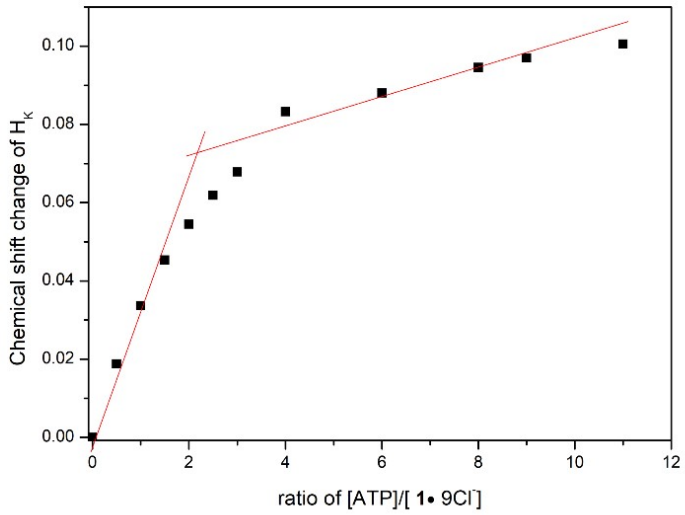

Fig S22. The variation curve of chemical shift for the complexation between **1**•9Cl$^-$ and ATP from ^{1}H NMR spectrum, indicating a 1:2 stoichiometry.

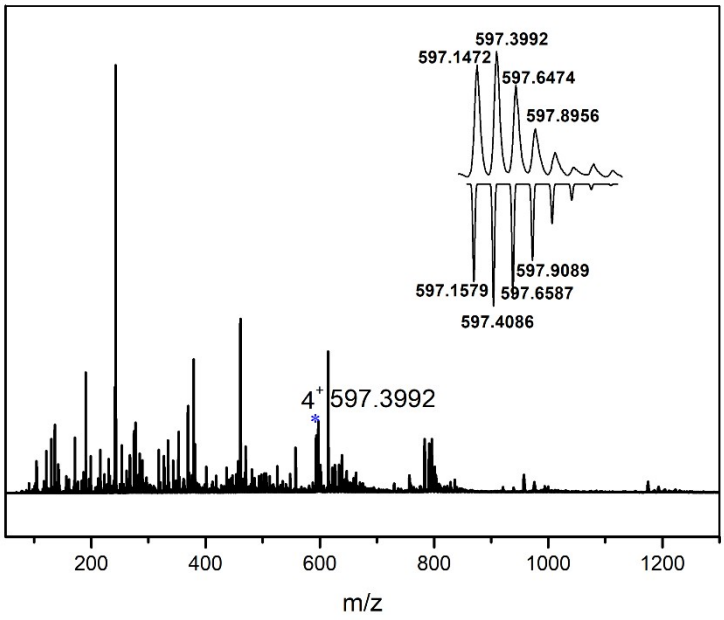

Fig S23. ESI-MS spectrum of **1**•9Cl$^-$⊃$(ATP)_2$.

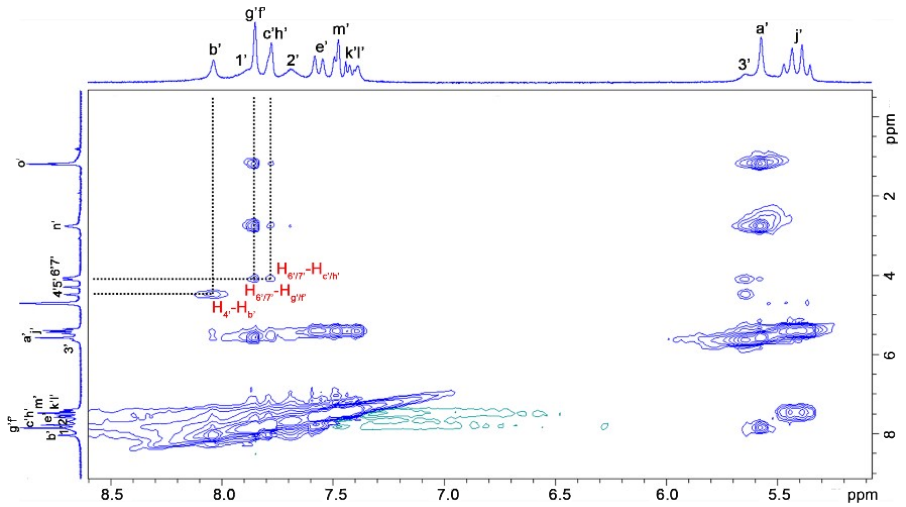

Fig. S24 NOESY spectrum (400 MHz, RT, D_2O) of **1**⊃ATP_2 ([**1**•9Cl^-]:[ATP] = 1:2).

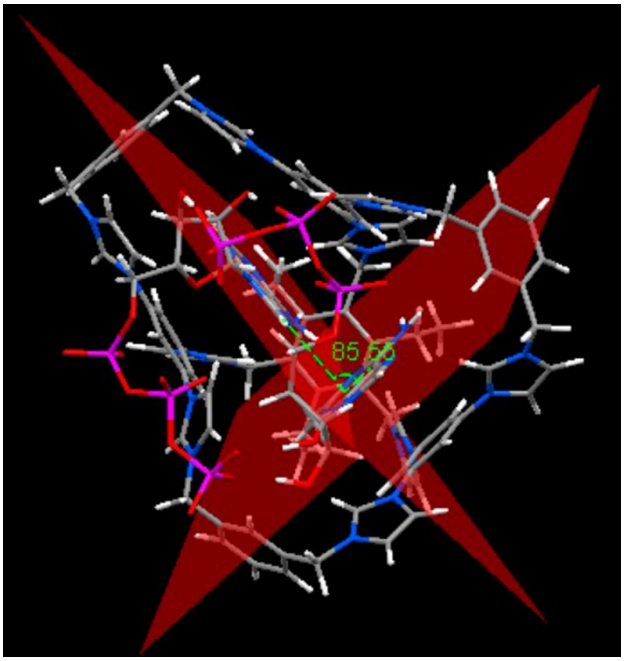

Fig. S25 The plane angle between two adenine groups of ATP in the energy-minimized structure of 1⊃ATP_2. Structure was optimized using DFT B3LYP-D3(BJ)/6-31G(d) with the default solvation model in water by Gaussian 16.

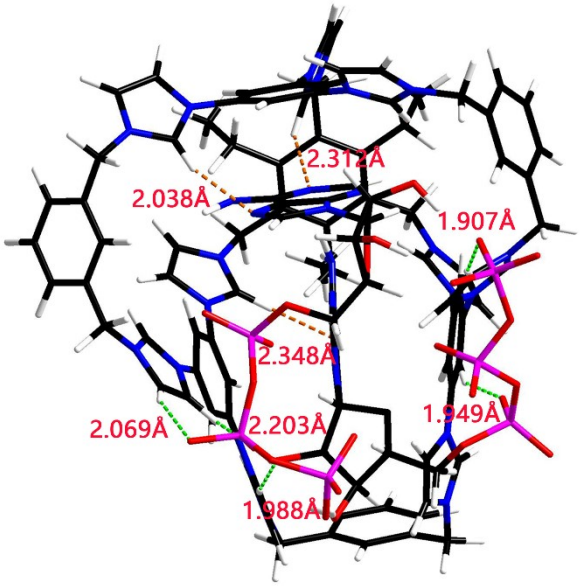

Fig. S26 The hydrogen bonds between the imidazolium C-H sites of host and the adenine and phosphate groups of guests. Structure was optimized using DFT B3LYP-D3(BJ)/6-31G(d) with the default solvation model in water by Gaussian 16.

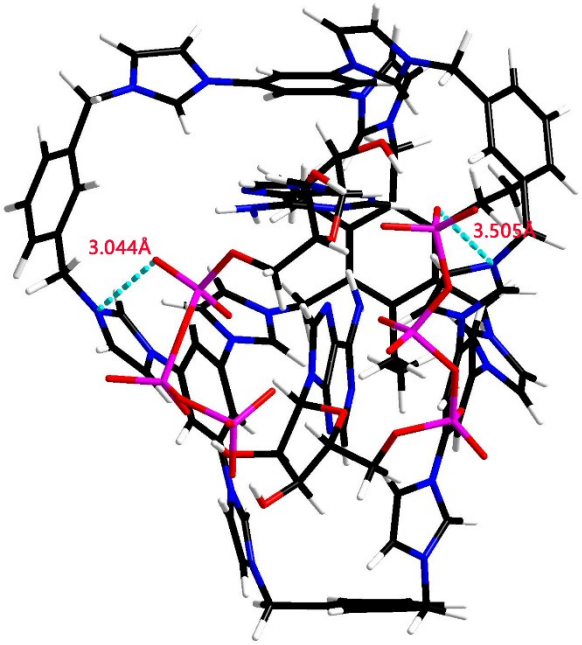

Fig. S27 The electrostatic interactions between the imidazolium rings of host and the phosphate groups of guests in the energy-minimized structure of **1**⊃ATP_2. Structure was optimized using DFT B3LYP-D3(BJ)/6-31G(d) with the default solvation model in water by Gaussian 16.

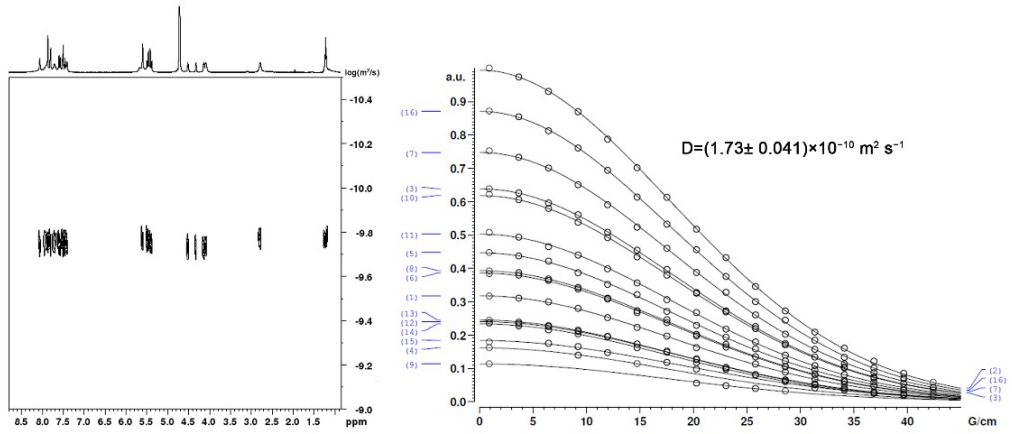

Fig. S28 DOSY spectrum (400 MHz, RT, D_2O) of **1**⊃ATP_2 ([**1**•9Cl^-]:[ATP] = 1:2).

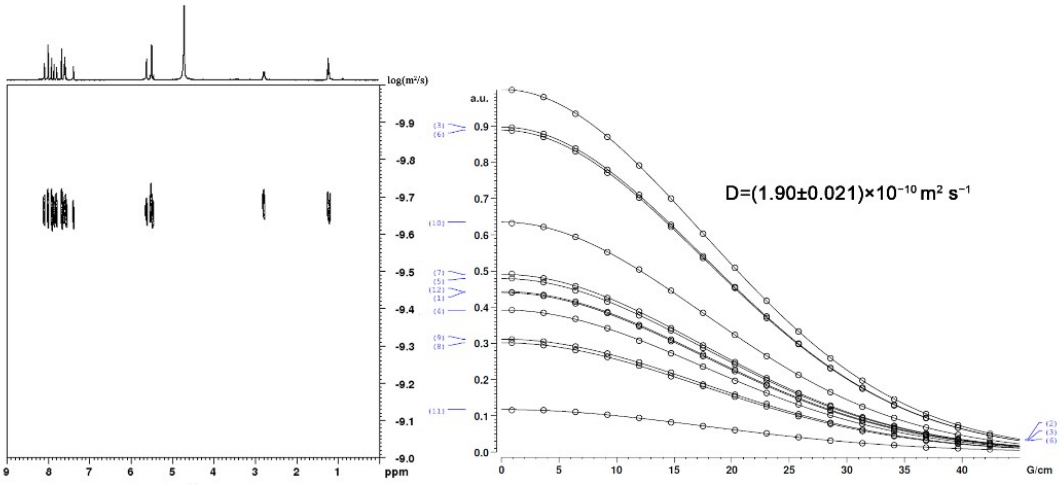

Fig. S29 DOSY spectrum (400 MHz, RT, D_2O) of **1**•9Cl^-.

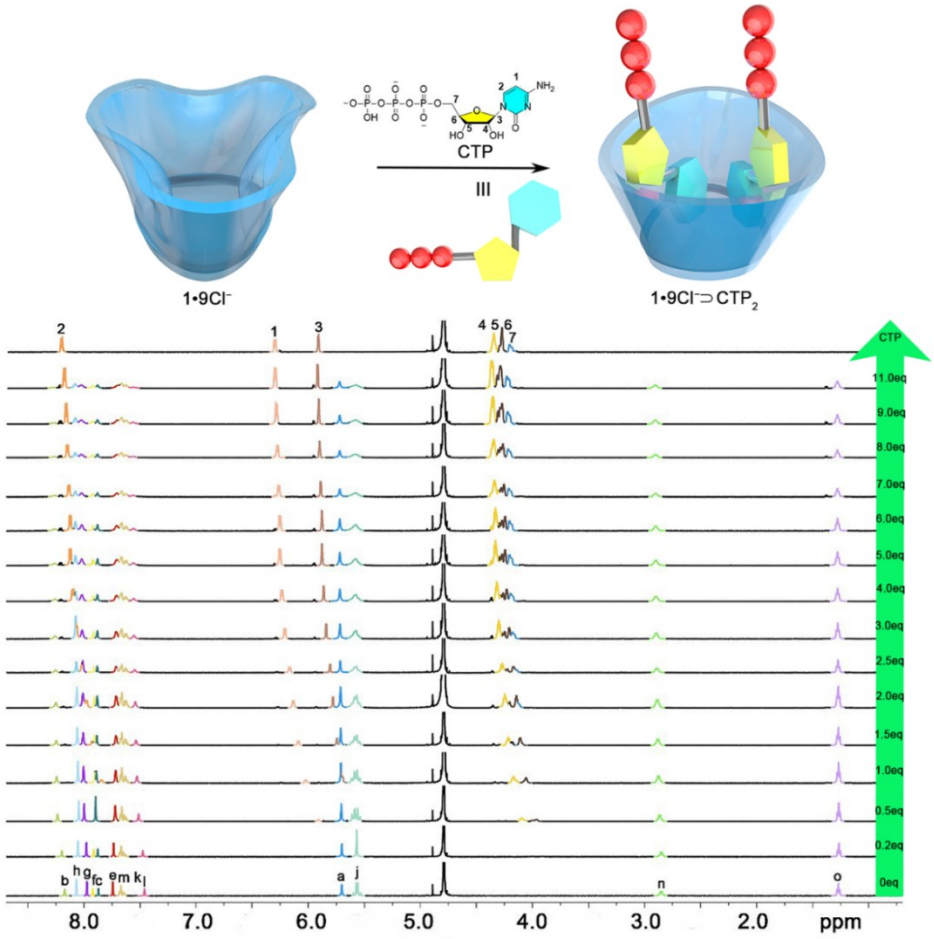

Fig. S30 ^{1}H NMR titration (600 MHz, RT, D_2O) of **1**•9Cl^- (1.0 mM) titrated by CTP (0-11.0 equiv).

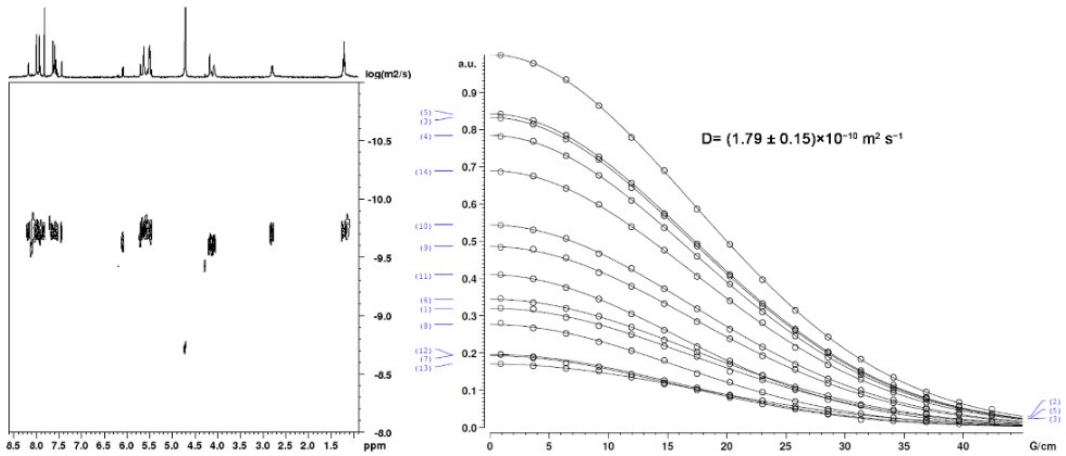

Fig. S31 DOSY spectrum (400 MHz, RT, D_2O) of **1**⊃CTP_2 ([**1**•9Cl^-]:[CTP] =1:2).

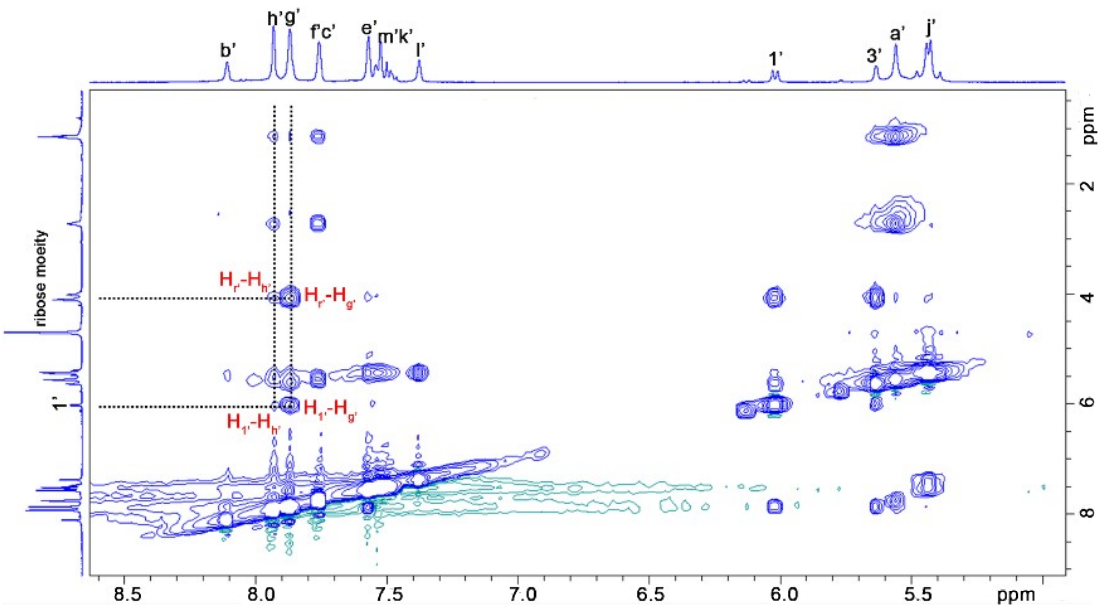

Fig. S32 NOESY spectrum (400 MHz, RT, D_2O) of **1**⊃CTP$_2$ ([**1**•9Cl$^-$]:[CTP] = 1:2).

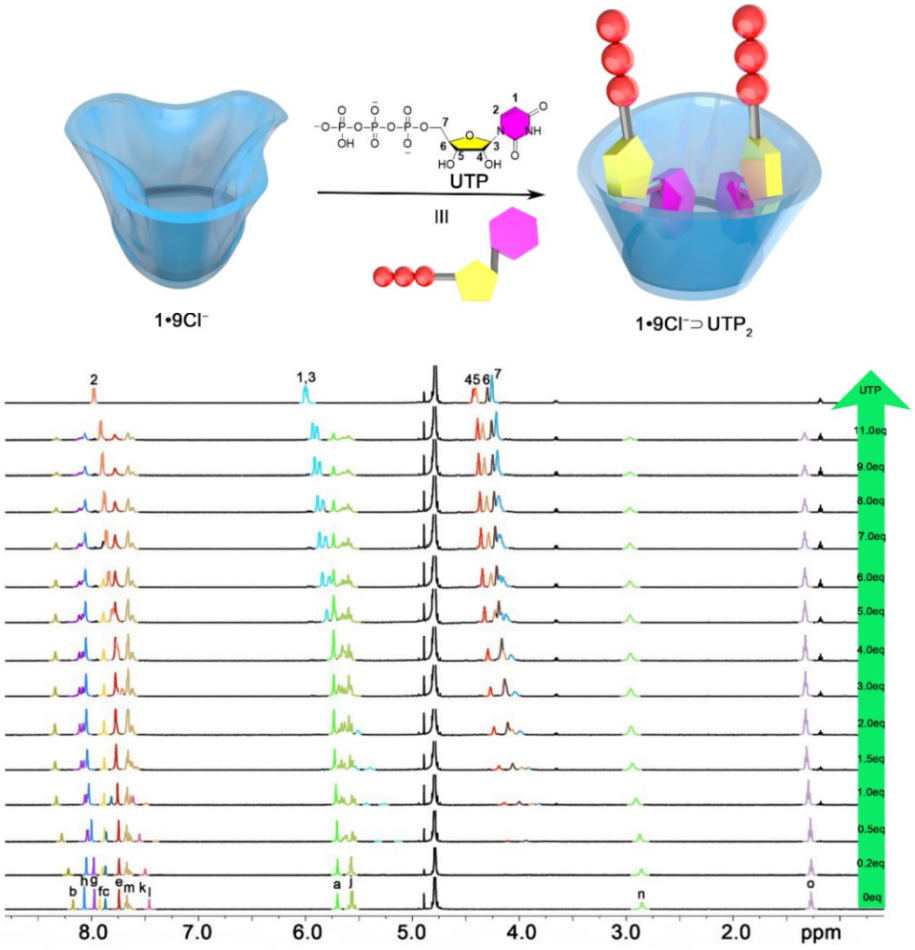

Fig. S33 ^{1}H NMR titration (600 MHz, RT, D_2O) of **1**•9Cl$^-$ (1.0 mM) titrated by UTP (0-11.0 equiv).

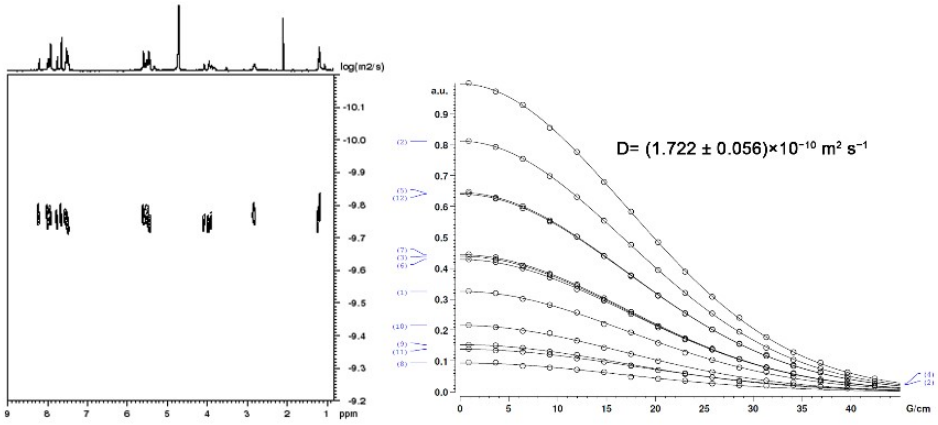

Fig. S34 DOSY spectrum (400 MHz, RT, D_2O) of **1**⊃UTP_2 ([**1**•9Cl^-]:[UTP] =1:2).

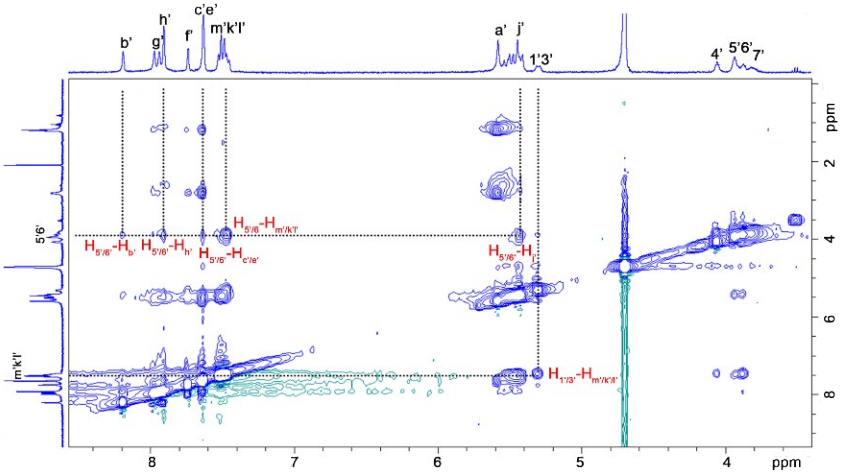

Fig. S35 NOESY spectrum (400 MHz, RT, D_2O) of **1**⊃UTP_2 ([**1**•9Cl^-]:[UTP] = 1:2).

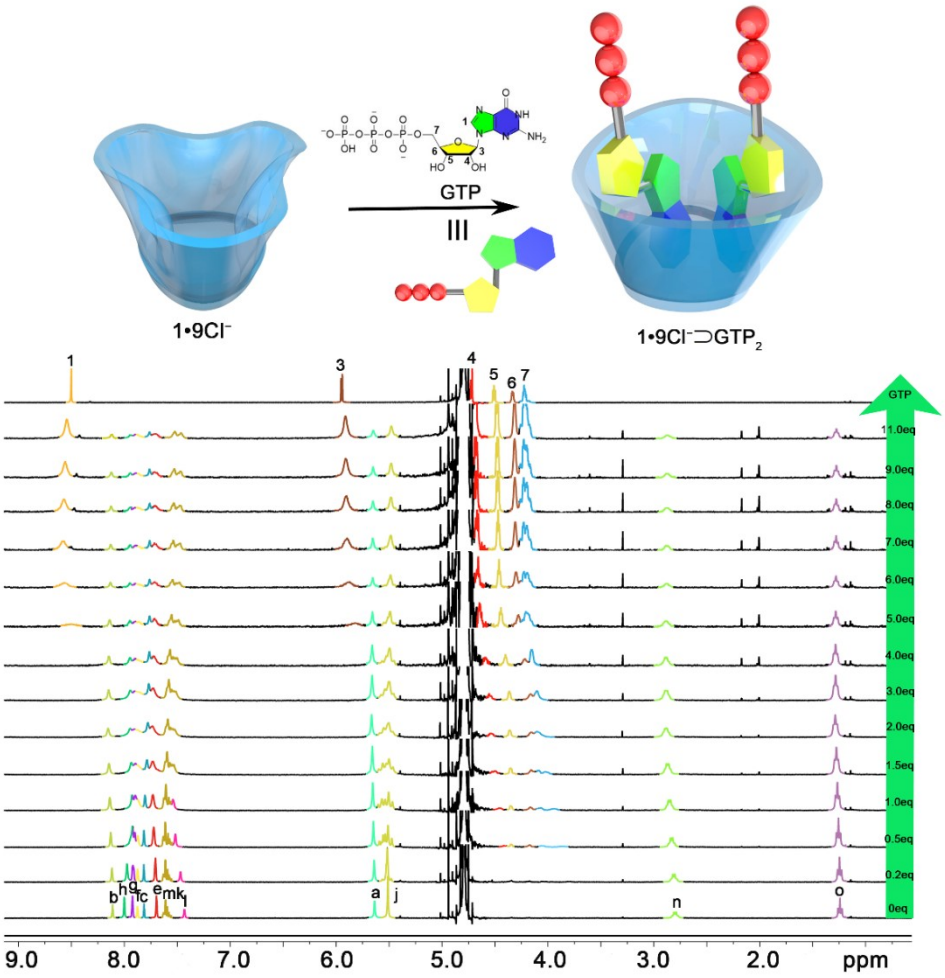

Fig. S36 ^{1}H NMR titration (400 MHz, RT, D_2O) of **1**•9Cl$^-$ (1.0 mM) titrated by GTP (0-11.0 equiv).

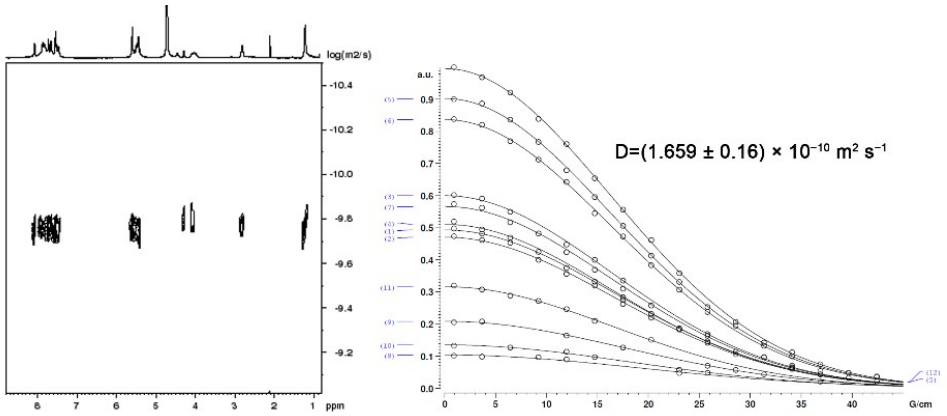

Fig. S37 DOSY spectrum (400 MHz, RT, D_2O) of **1**⊃GTP_2 ([**1**•9Cl$^-$]:[GTP] =1:2).

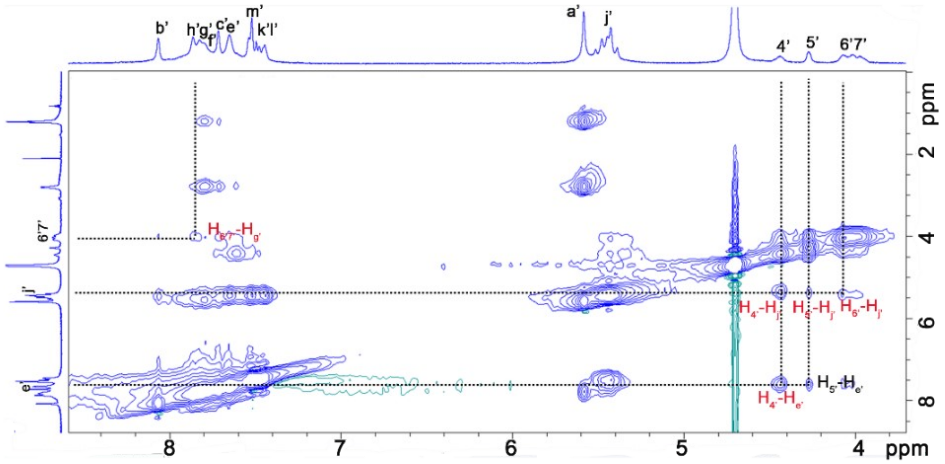

Fig. S38 NOESY spectrum (400 MHz, RT, D_2O) of **1**⊃GTP_2 ([**1**•9Cl^-]:[GTP] = 1:2).

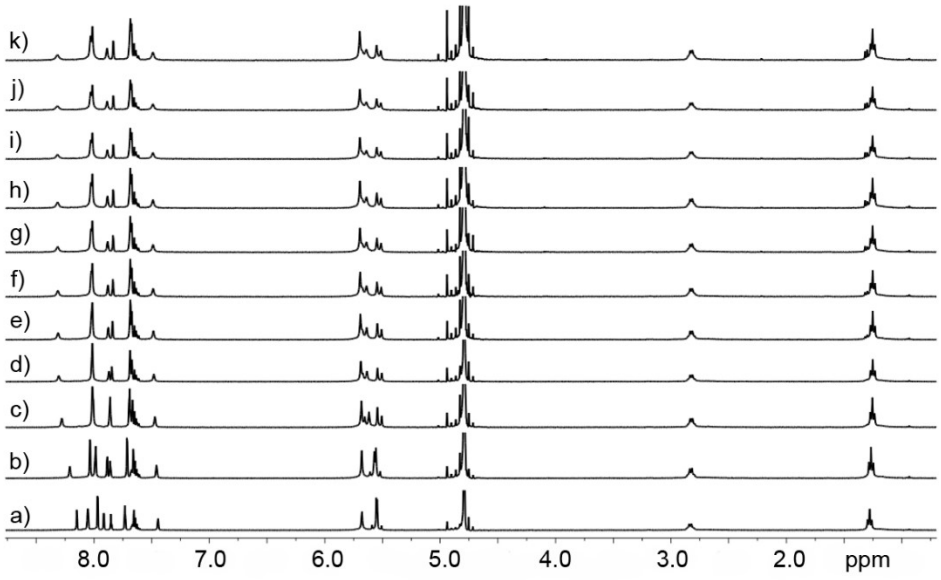

Fig. S39 ^1H NMR titration (400 MHz, RT, D_2O) of (a) **1**•9Cl^- (0.8 mM); (b-k) 0.25-6.0 equiv of pyrophosphate.

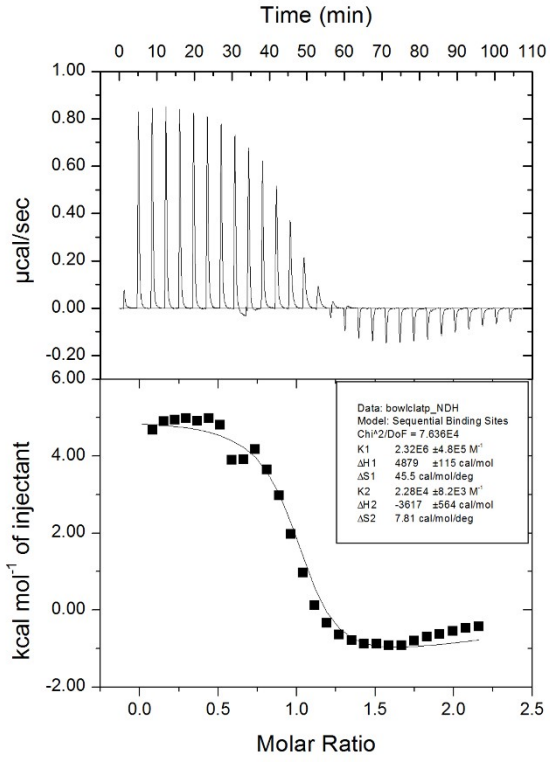

Fig. S40 ITC titration of **1**•9Cl^{-} (0.05 mM) with ATP (0.75 mM) in aqueous solution.

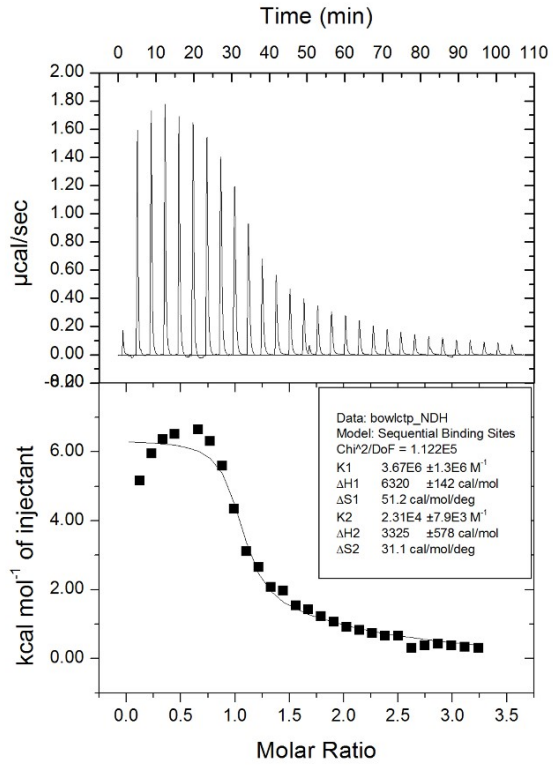

Fig. S41 ITC titration of **1**•9Cl^{-} (0.05 mM) with CTP (0.75 mM) in aqueous solution.

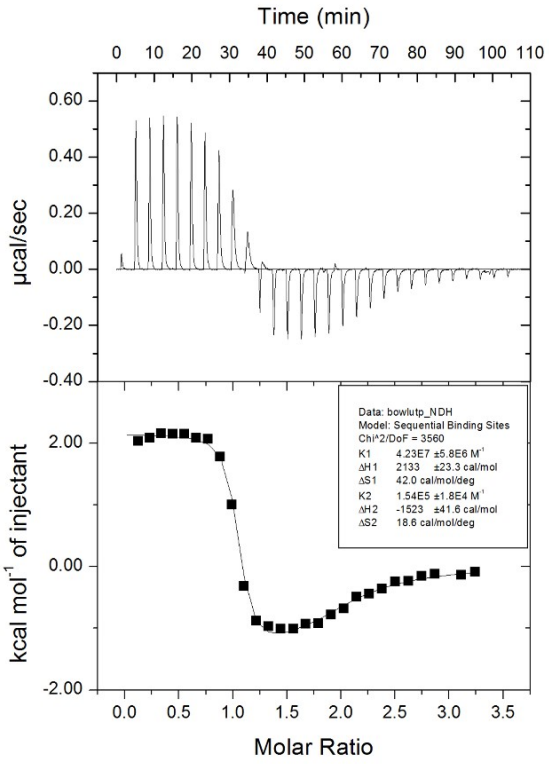

Fig. S42 ITC titration of **1**•9Cl^{-} (0.05 mM) with UTP (0.75 mM) in aqueous solution.

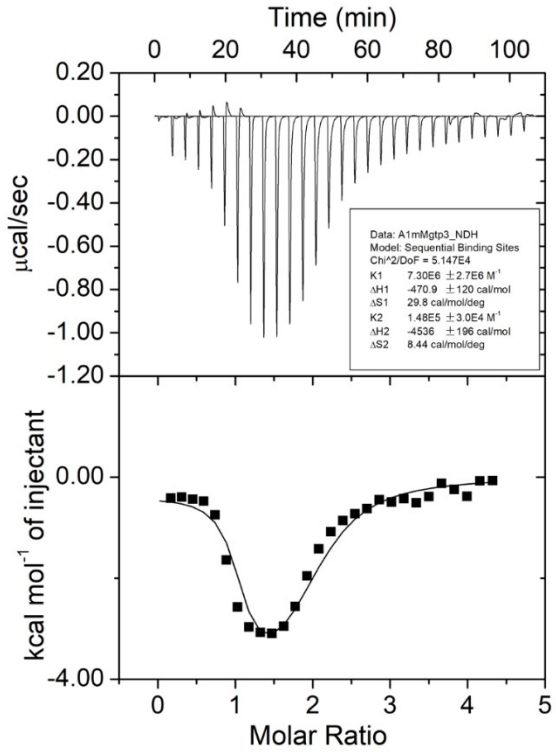

Fig. S43 ITC titration of **1**•9Cl^{-} (0.05 mM) with GTP (0.75 mM) in aqueous solution.

Table S3 The calculated binding constants (K_a) of **1**•9Cl$^-$ with nucleotides from ITC data in water.

Anion	Stoichiometry (Host:Guest)	K_1/M^{-1}	K_2/M^{-1}
ATP	1:2	(2.32±0.48)×10^6	(2.28±0.82)×10^4
CTP	1:2	(3.67±0.13)×10^6	(2.31±0.79)×10^4
UTP	1:2	(4.23±0.58)×10^7	(1.54±0.18)×10^5
GTP	1:2	(7.30±2.37)×10^6	(1.48±0.30)×10^4

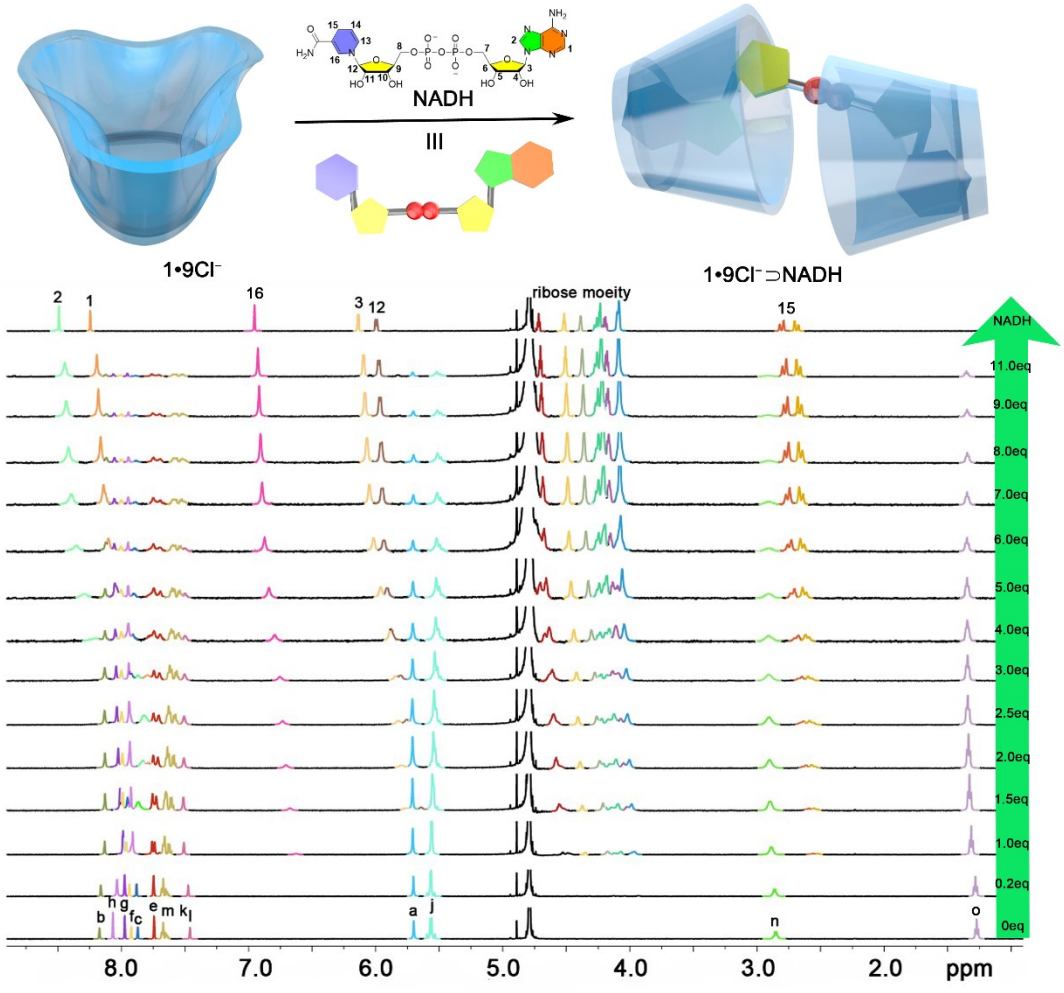

Fig. S44 ^{1}H NMR titration (400 MHz, RT, D_2O) of **1**•9Cl$^-$ (1.0 mM) titrated by NADH (0-11.0 equiv).

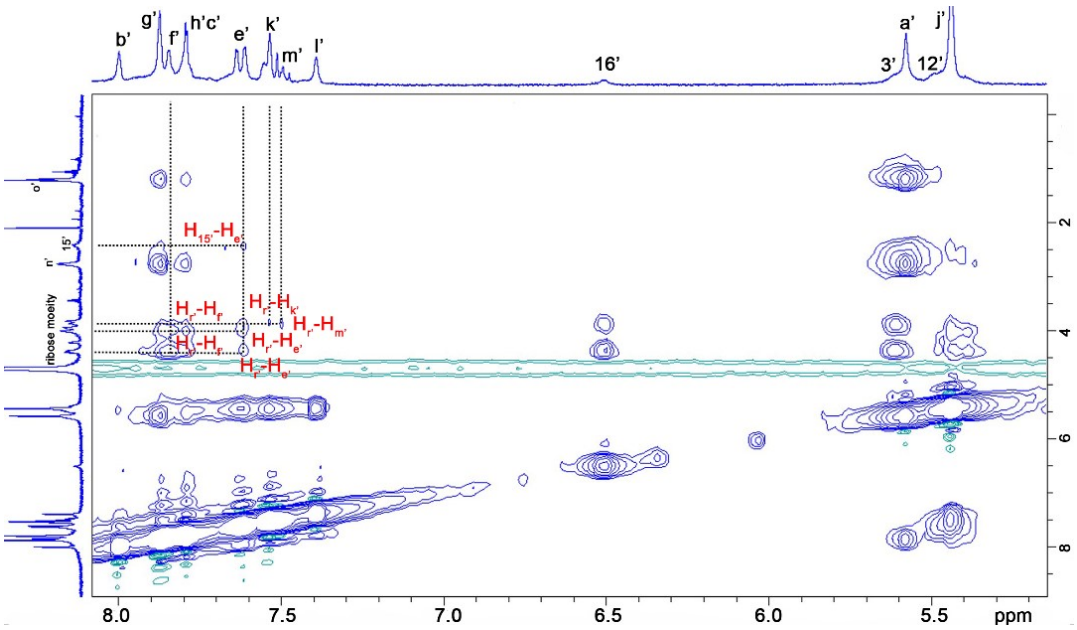

Fig. S45 NOESY spectrum (400 MHz, RT, D_2O) of $\mathbf{1}_2$⊃NADH ([1•9Cl$^-$]:[NADH] = 2:1).

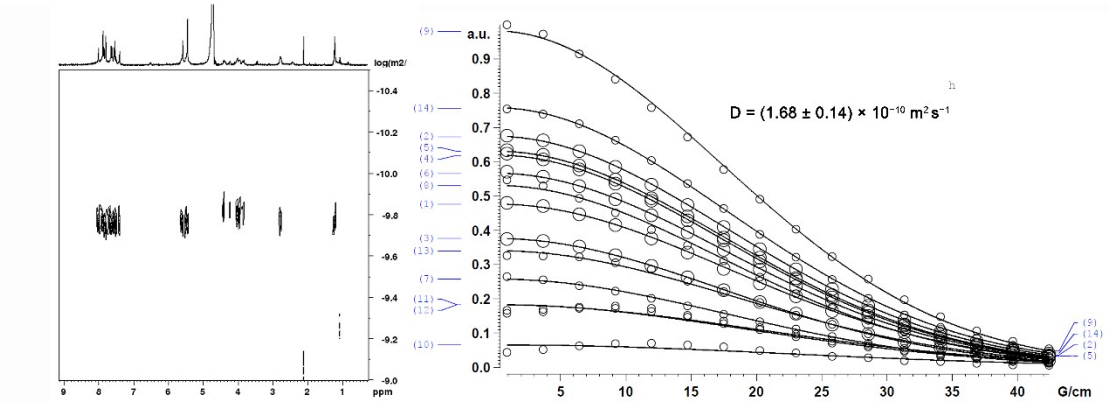

Fig. S46 DOSY spectrum (400 MHz, RT, D_2O) of $\mathbf{1}_2$⊃NADH ([**1**•9Cl$^-$]:[NADH] = 2:1).